Supporting Information

Eigth at one Stroke – A Synthetic Tetra-Disulfide Peptide Epitope

Andreas Schrimpf,[a] *Uwe Linne*[b] *and Armin Geyer*[a]

[a]Department of Chemistry, Philipps-Universität Marburg, Hans-Meerwein-Straße 4, 35032 Marburg, E-mail: geyer@staff.uni-marburg.de
[b]Mass spectrometry facility of the Department of Chemistry, Philipps-Universität Marburg, 35032 Marburg, E-mail: linneu@staff.uni-marburg.de

Table of Contents

Peptide Synthesis

Resin Loading

2-Chlorotritylchloride resin (1.60 mmol/g) was loaded with Fmoc-Cys(Trt)-OH by adding the protected amino acid (1.50 eq) and DIPEA (6.00 eq) in DMF (10 mL/g resin) and stirring for 5 h. After washing the resin with DMF, methanol and DCM several times, the resin was treated with a mixture of DCM/methanol/DIPEA (80:15:5) two times for 30 min and washed several times with DMF, methanol and DCM before it was dried under vacuum. The loading of the used resins was estimated to be between 0.50 mmol/g and 0.60 mmol/g by UV-Vis spectroscopy at 289 nm and 300 nm after cleaving the Fmoc protecting group with 20% piperidine in DMF for 20 min.

Solid Phase Peptide Synthesis

Peptides were synthesised on a microwave assisted peptide synthesiser (*Liberty Blue, CEM*). Fmoc-strategy was applied. The 2CTC-resins loaded with Fmoc-Cys(Trt)-OH (scheduled quantity: 0.1 mmol, 1.00 eq) ran through the following cycles of Fmoc-deprotection and amino acid coupling:

- **Fmoc-deprotection**: T = 50 °C, $P_{microwave}$ = 30 W, t = 210 s with piperidine (20 w% in DMF, 3.00 mL/deprotection)

- **Amino acid coupling**:
  - for amino acids except Fmoc-Arg(Pbf)-OH:
    T = 50 °C, $P_{microwave}$ = 30 W, t = 600 s with Fmoc-protected amino acid (0.2 M in DMF, 5.00 eq, 2.5 mL/coupling), DIC (0.5 M in DMF, 5.00 eq, 1 mL/coupling) and Oxyma (1 M in DMF, 5.00 eq, 0.5 mL)
  - for Fmoc-Arg(Pbf)-OH:
    1. T = 25 °C, $P_{microwave}$ = 0 W, t = 1500 s
    2. T = 50 °C, $P_{microwave}$ = 35 W, t = 660 s

    with Fmoc-protected amino acid (0.2 M in DMF, 5.00 eq, 2.5 mL/coupling), DIC (0.5 M in DMF, 5.00 eq, 1 mL/coupling) and Oxyma (1 M in DMF, 5.00 eq, 0.5 mL)

Resin Cleavage

Resin cleavage was performed with a mixture of TFA/H_2O/phenol/TIPS (88:4:4:4) for 300 min. Peptides were precipitated from cold diethyl ether (40 mL), washed two to three times with diethyl ether and lyophilised from water.

Disulfide Formation

Crude lyophilised peptides were dissolved in water and the resulting solution was brought to pH 8.4 with $(NH_4)_2CO_3$ (c ≈ 1 mg/mL). The progress of the oxidation was monitored via analytical HPLC. After completion, the solution was lyophilised.

Purification

Peptides were purified by semi-preparative reversed-phase HPLC on a *Thermo Fisher Ultimate 3000 LC System* with the following parameters:

Column: ACE5 SuperC18, 150 mm x 10 mm id
Gradient: 15-30% B in 20 min (A: water + 0.1% TFA, B: acetonitrile + 0.85% TFA)
Flow rate: 7.00 mL/min

Isolated yields of peptides from 100 mg of crude peptide:

- Dimer **1d**: 16 mg
- Dimer **1d-Ahx**: 12 mg
- Monomer **2m**: 8 mg
- Dimer **2d**: 8 mg

} obtained in one run from the same crude peptide

- Monomer **3m-Ahx**: 5 mg
- Dimer **3d**: 8 mg

Analytics

Table S1. Peptide sequences, HPLC retention times (rt; chromatographic details are given in figures S15-S23) and ESI-MS results.

Peptide	Sequence	rt / min	m/z (calculated)	m/z (ESI-MS)
1d	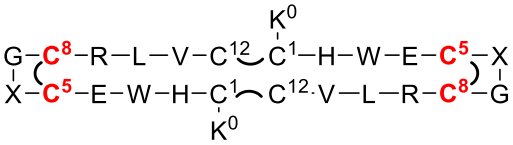	7.15	795.8341 $[M+4H]^{4+}$	795.8344 $[M+4H]^{4+}$
1d-Ahx	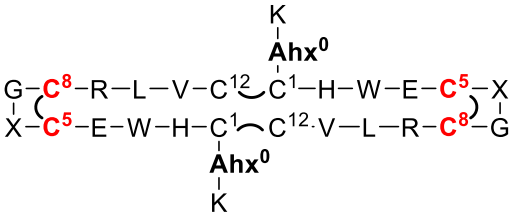	7.57	852.3762 $[M+4H]^{4+}$	852.3770 $[M+4H]^{4+}$
2m	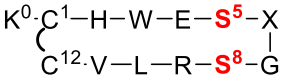	6.02	780.3639 $[M+2H]^{2+}$	780.3639 $[M+2H]^{2+}$
2d	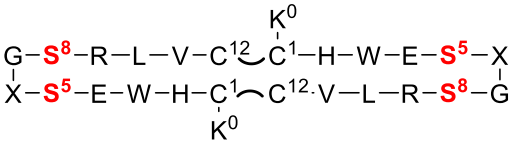	6.30	780.6146 $[M+4H]^{4+}$	780.6148 $[M+4H]^{4+}$
3m-Ahx	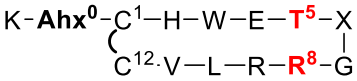	6.42	585.9680 $[M+5H]^{5+}$	585.9673 $[M+5H]^{5+}$
3d	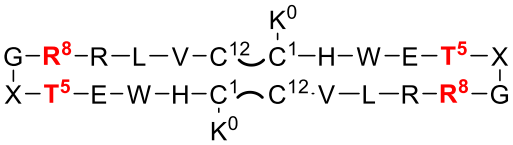	6.00	1095.8735 $[M+3H]^{3+}$	1095.8736 $[M+3H]^{3+}$

Mass Spectrometry

Mass spectra (ESI+) were acquired on a *Thermo Fisher Scientific LTQ-FT*. The exact mass spectra as well as charge and isotope pattern allow a differentiation between monomers and dimers.

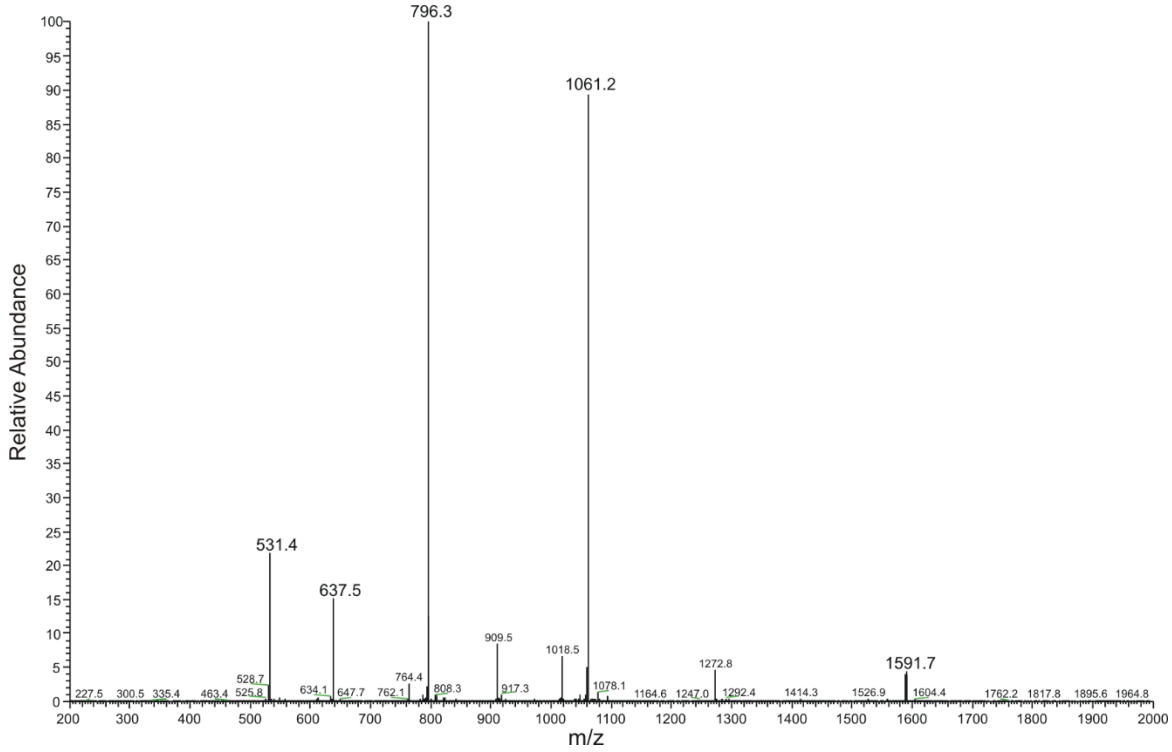

Figure S1. Mass spectrum with charge pattern m/z of tetra-disulfide dimer **1d**.

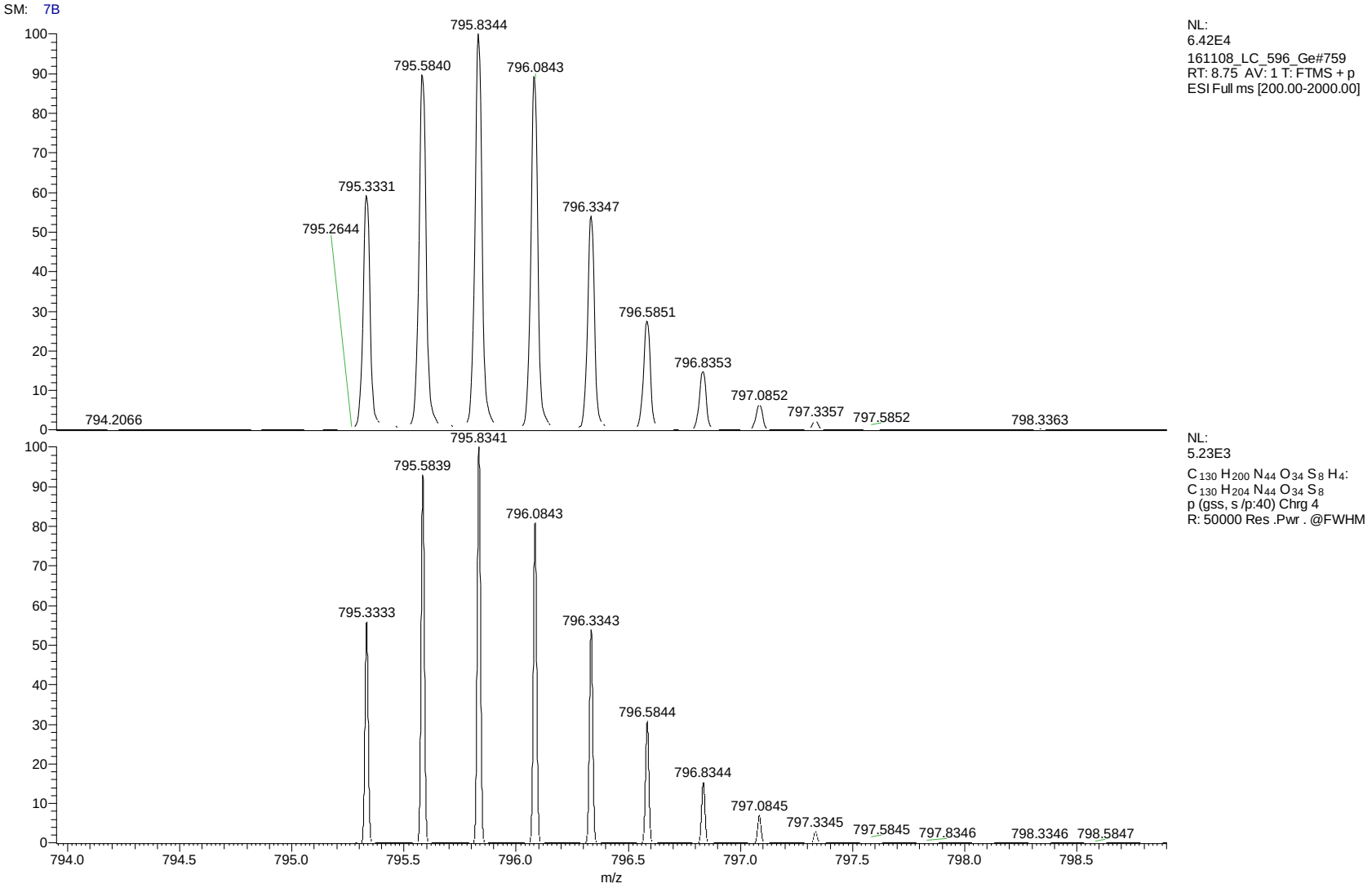

Figure S2. High resolution mass spectrum with isotope pattern of peptide **1d**.

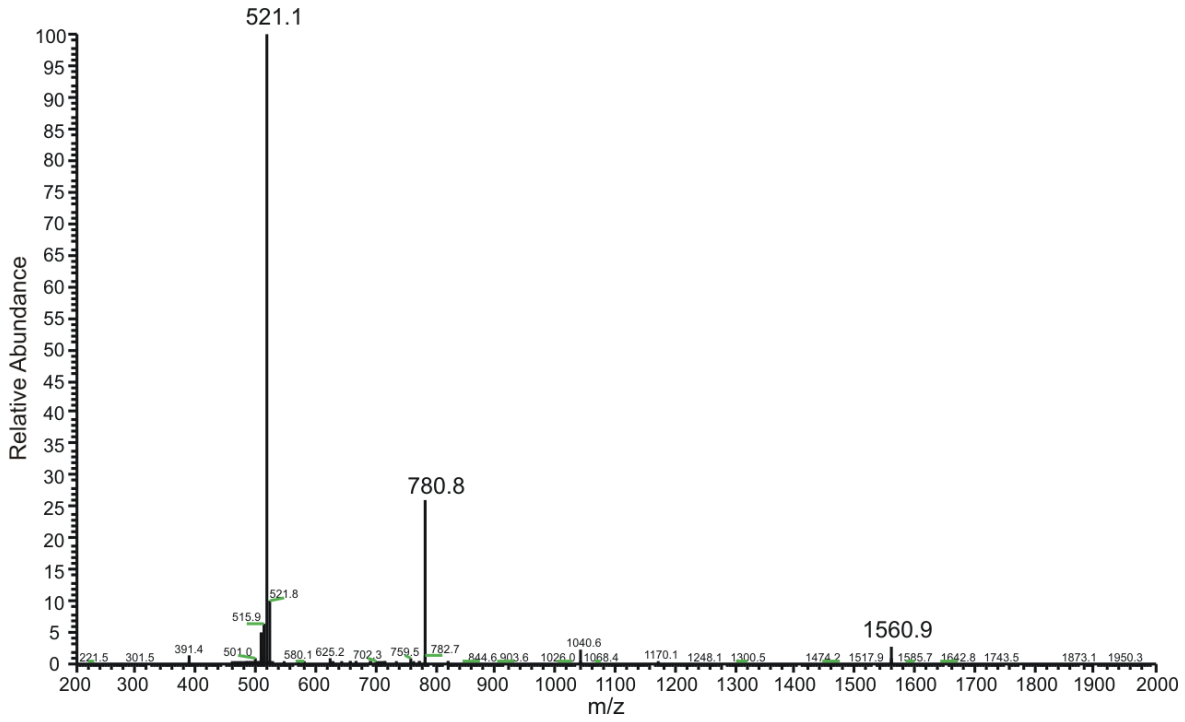

Figure S3. Mass spectrum with charge pattern m/z for monomer **2m**.

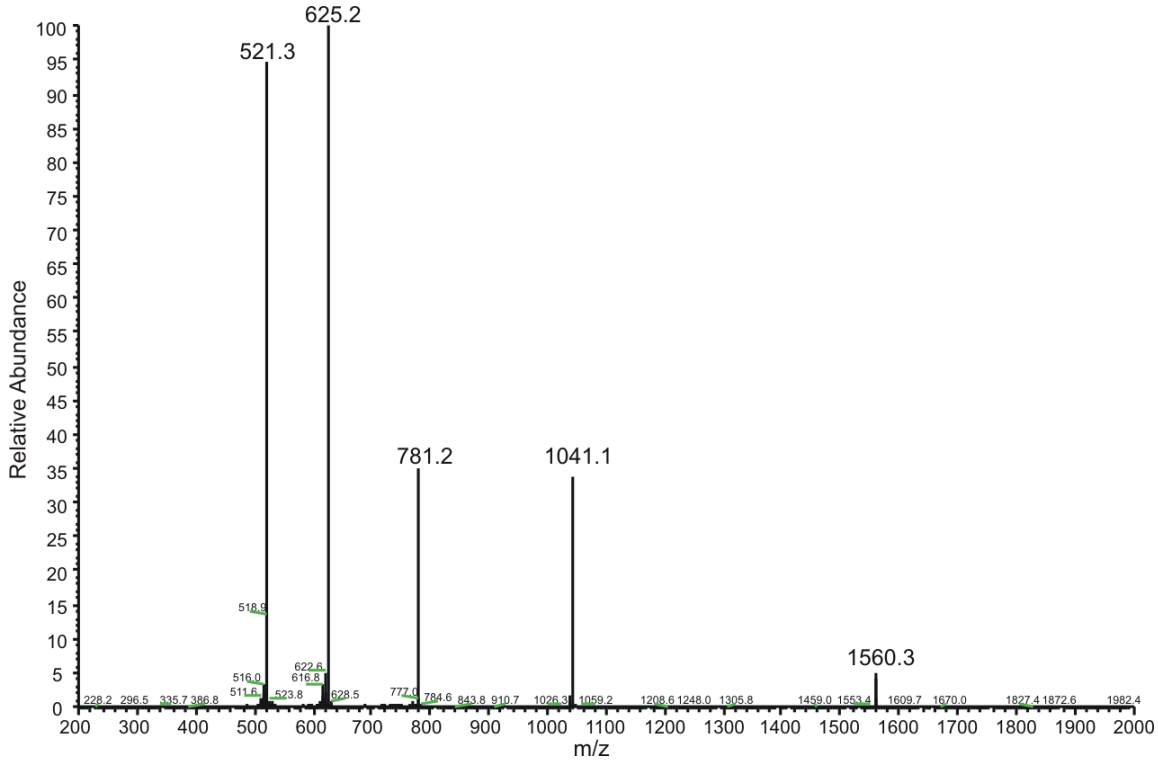

Figure S4. Mass spectrum with charge pattern m/z for monomer **2d**.

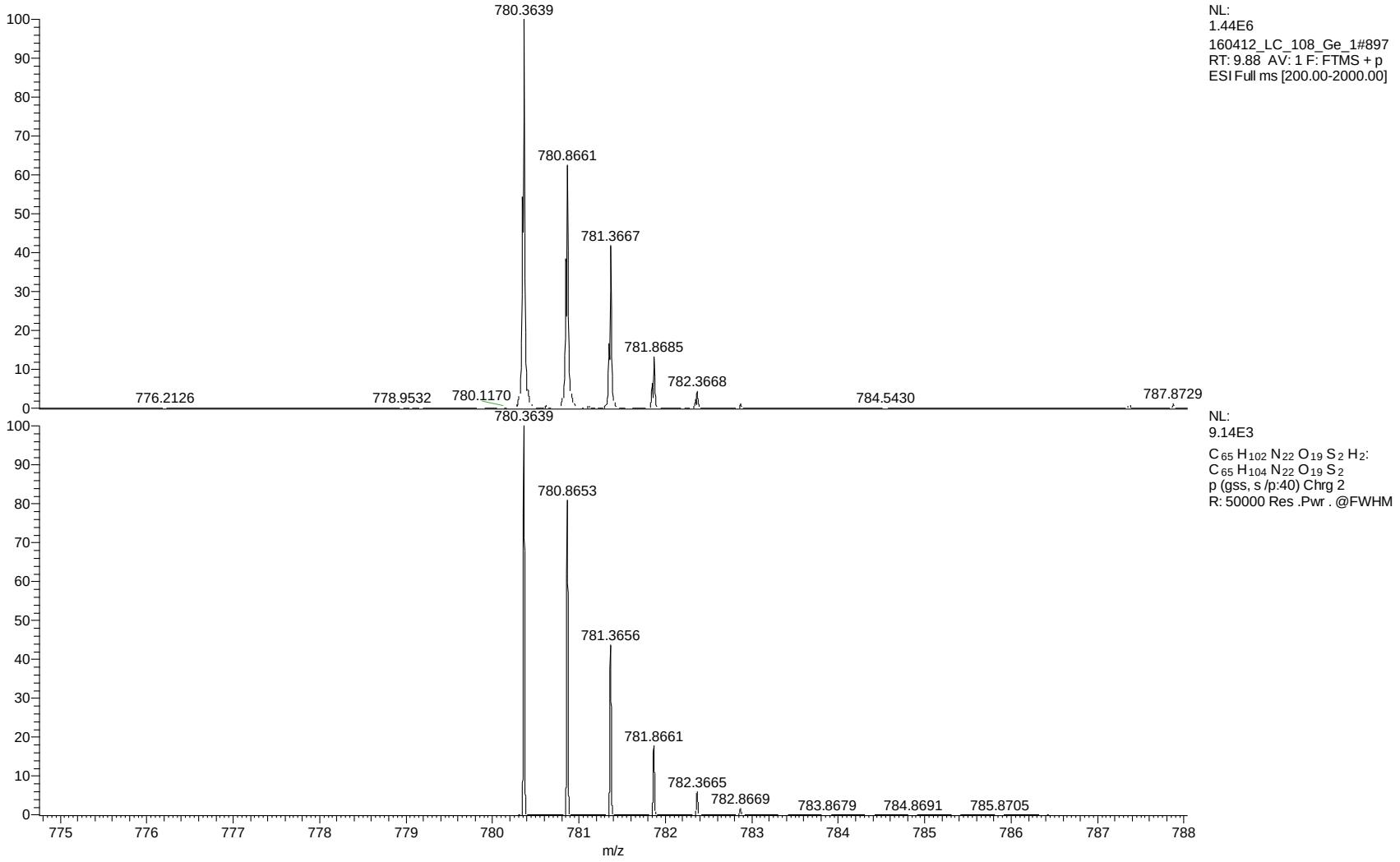

Figure S5. High resolution mass spectrum with isotope pattern of peptide **2m**.

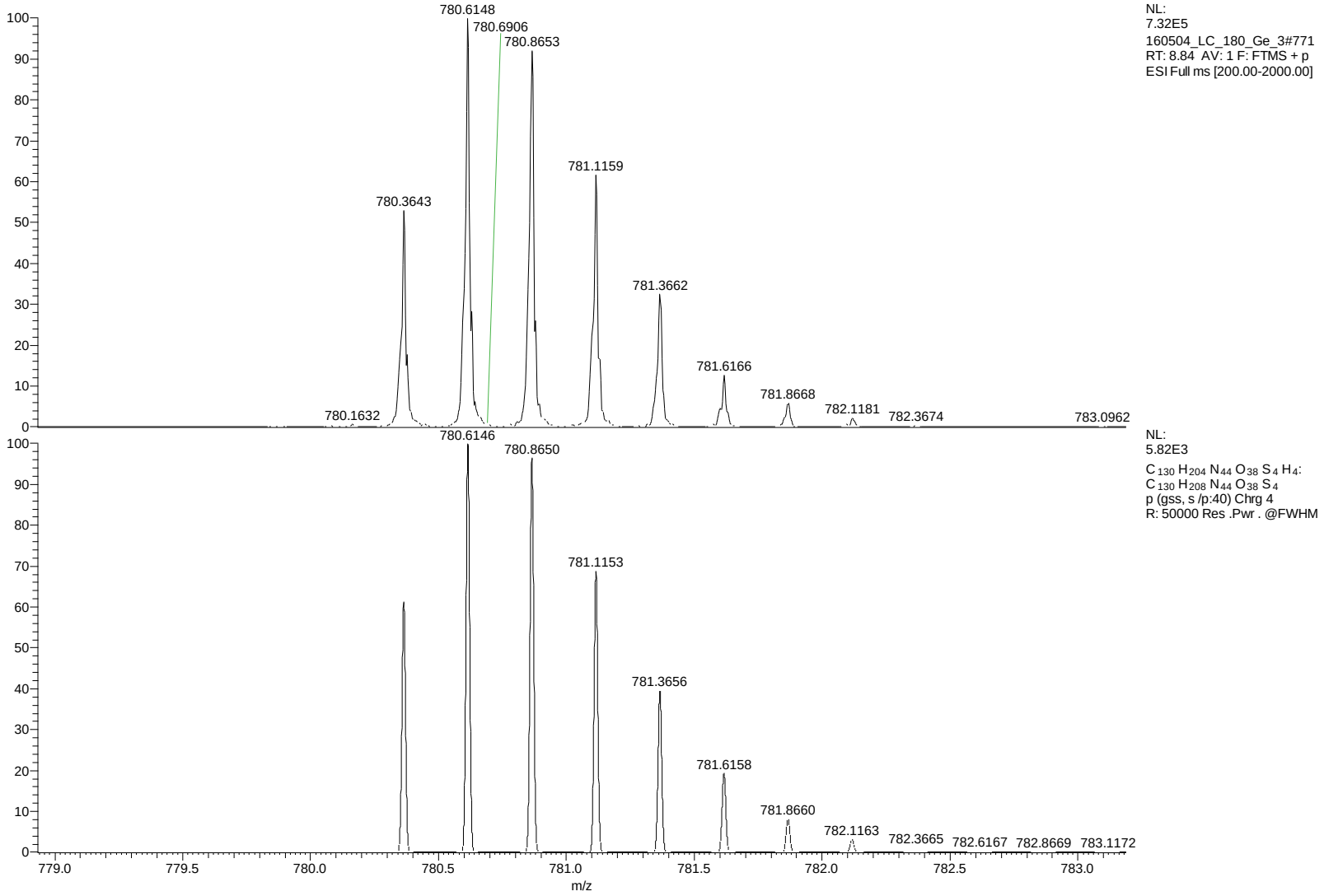

Figure S6. High resolution mass spectrum with isotope pattern of peptide **2d**.

Trypsin Degradation

For enzymatic degradation, a few micrograms of the peptide dimers were dissolved in NH_4CO_3 buffer (50 mM, pH = 8.0) and an excess of trypsin was added. After 5 min at 37 °C, the digestion was stopped by addition of 2 µL of formic acid. The solution was then directly applied to LC-MS measurements.

We searched for fragments with intact disulfide bridges but broken amide bonds (figure S7). Thus, we could distinguish fragments that are linked between C1-C1/C12-C12 or C1-C12/C1-C12 respectively. A typical mass spectrum with corresponding chromatograms is shown for peptide dimer **2d** (S5,S8). Only C1-C12/C1-C12 connections were observed with no intact dimeric species left. For tetra-disulfide **1d**, no relevant fragments were found, but the intact dimer could be identified.

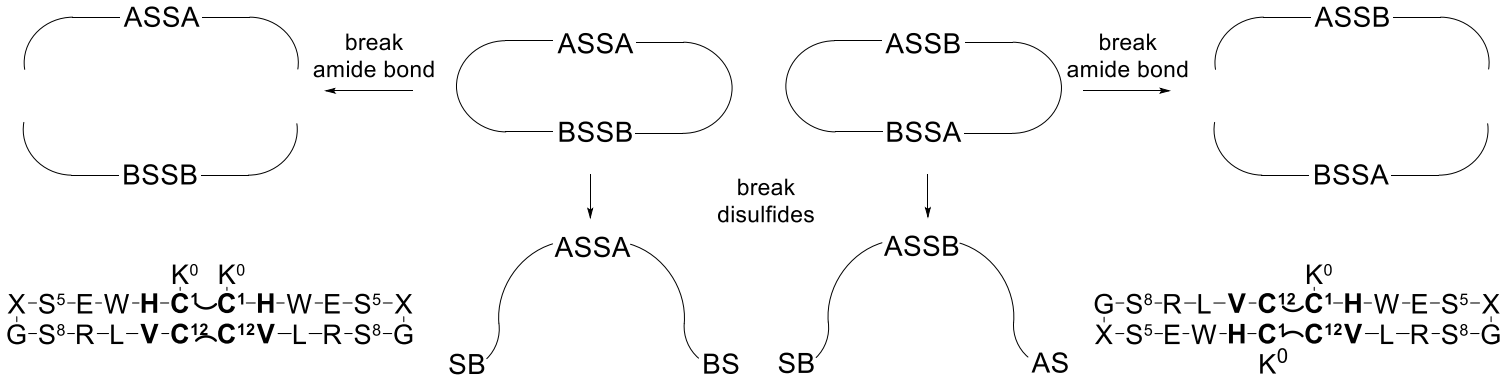

Figure S7. Possible disulfide connection patterns and their fragmentation pattern when disconnected at the disulfide or the amide bonds.

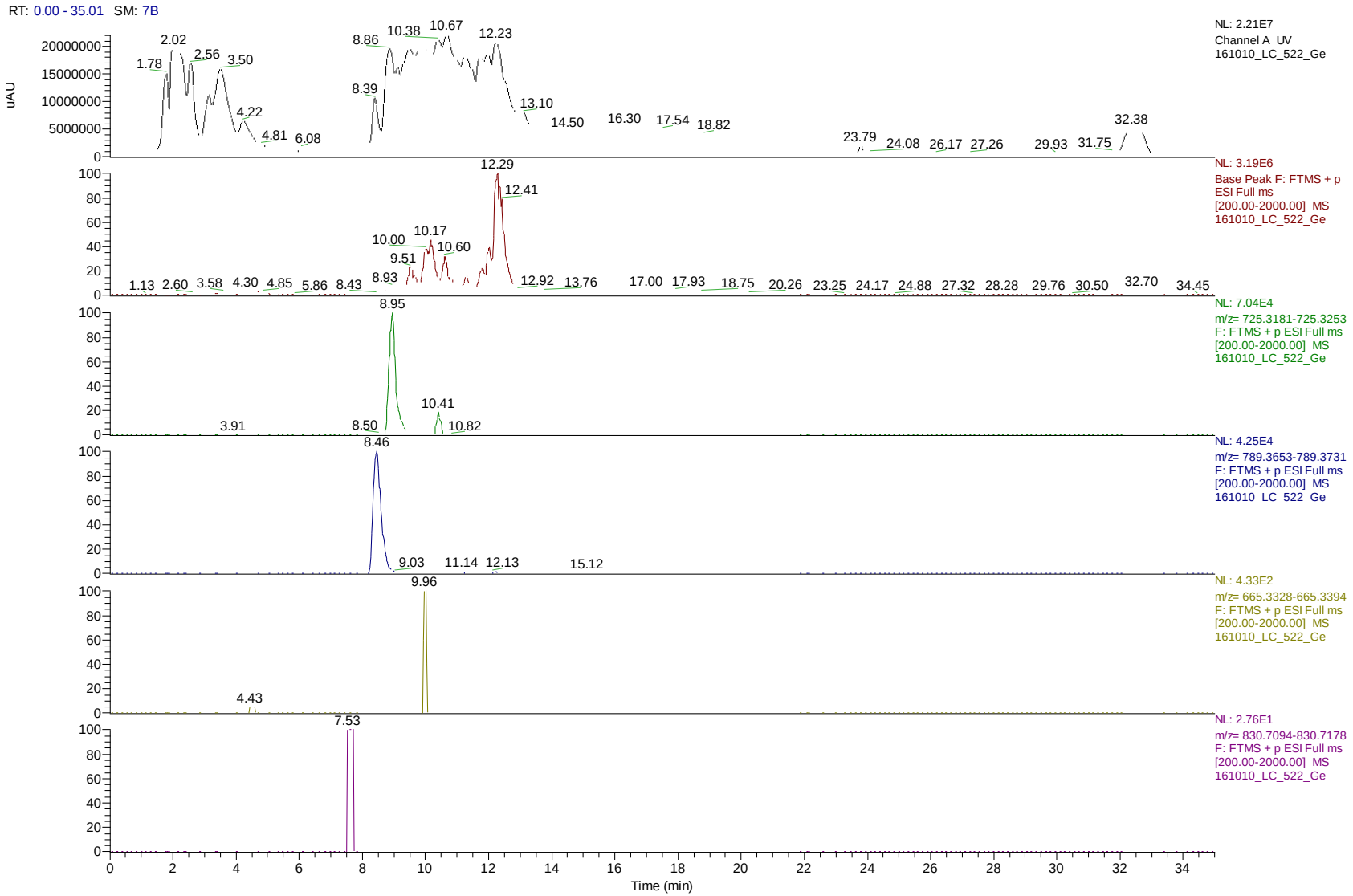

Figure S8. LC-MS chromatograms of peptide dimer **2d** after digestion with trypsin.

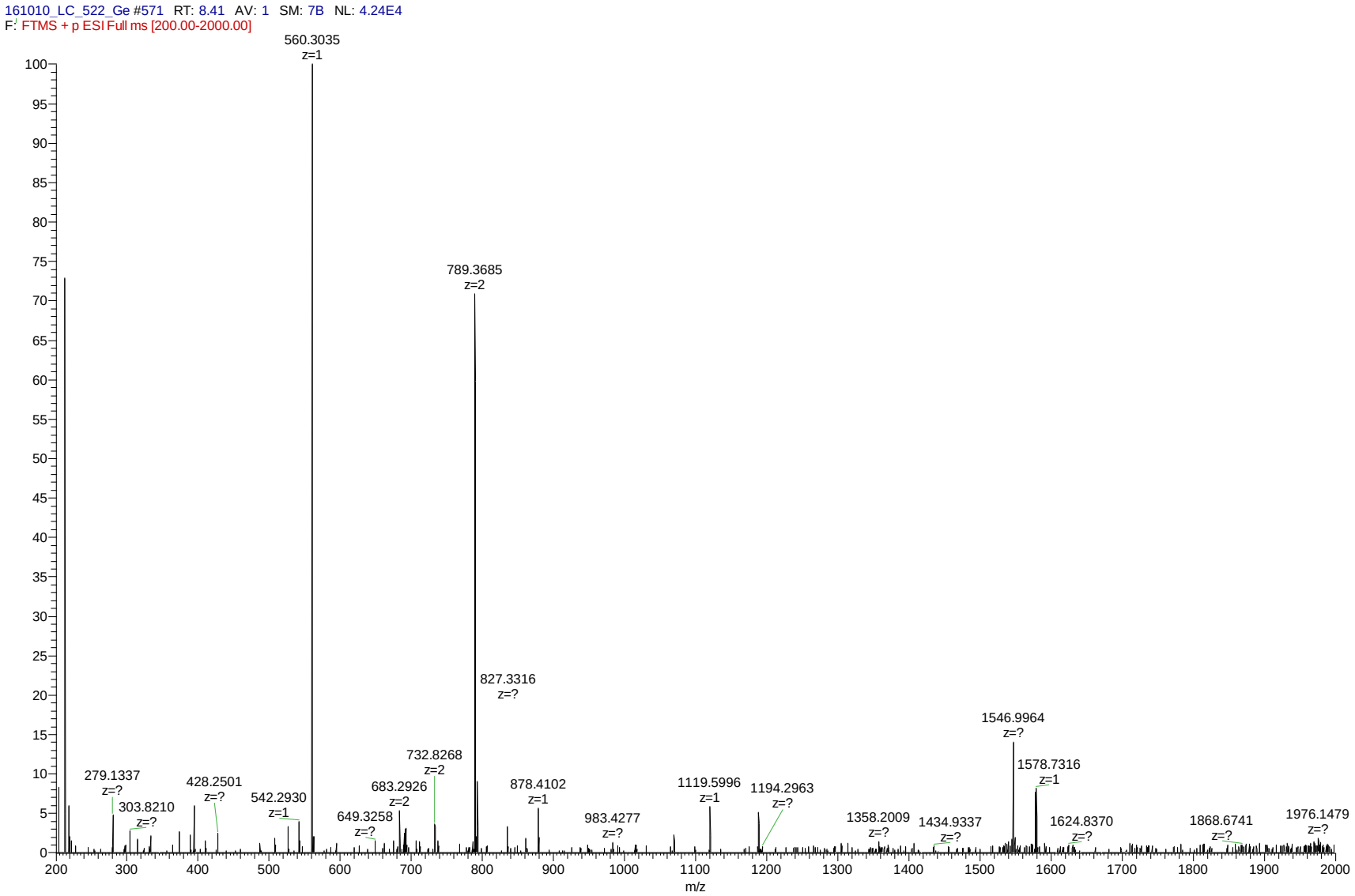

Figure S9. Mass spectrum of fragments from trypsin degradation of peptide dimer **2d**. Intact dimeric species cannot be identified.

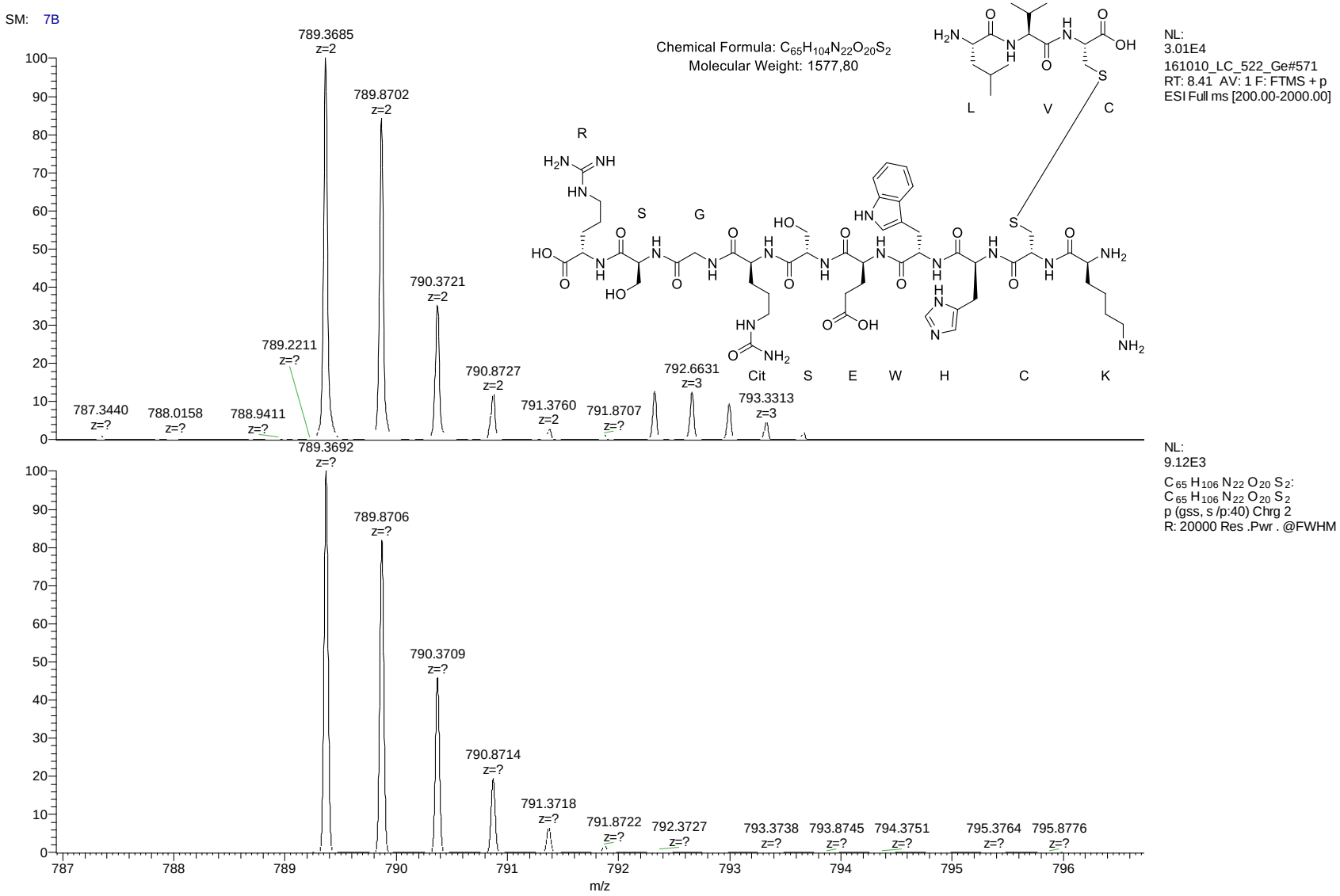

Figure S10. High resolution mass spectrum of the shown C1-C12/C1-C12 connected fragment of peptide dimer **2d**.

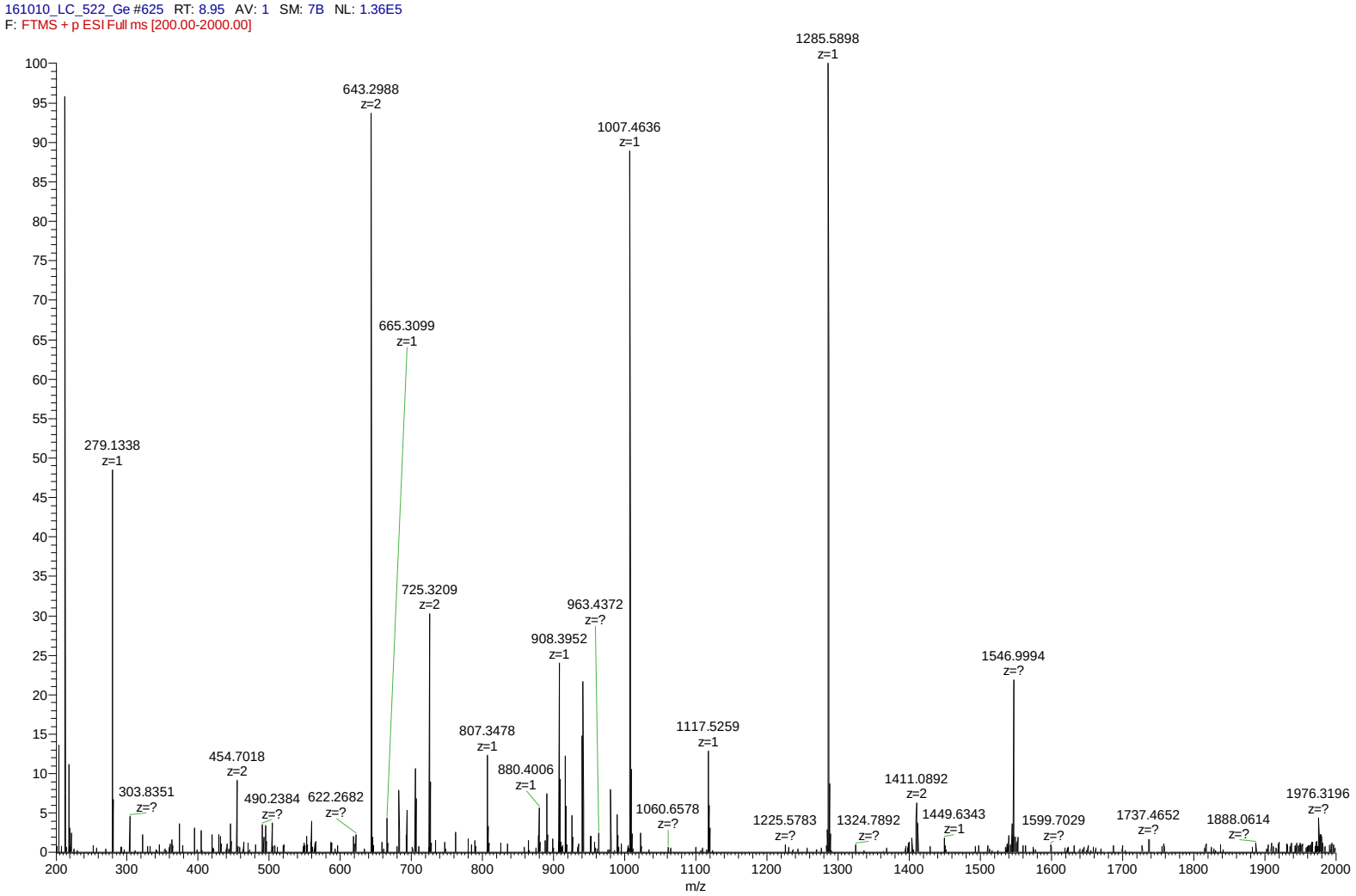

Figure S11. Mass spectrum of fragments from trypsin degradation of peptide dimer **2d**.

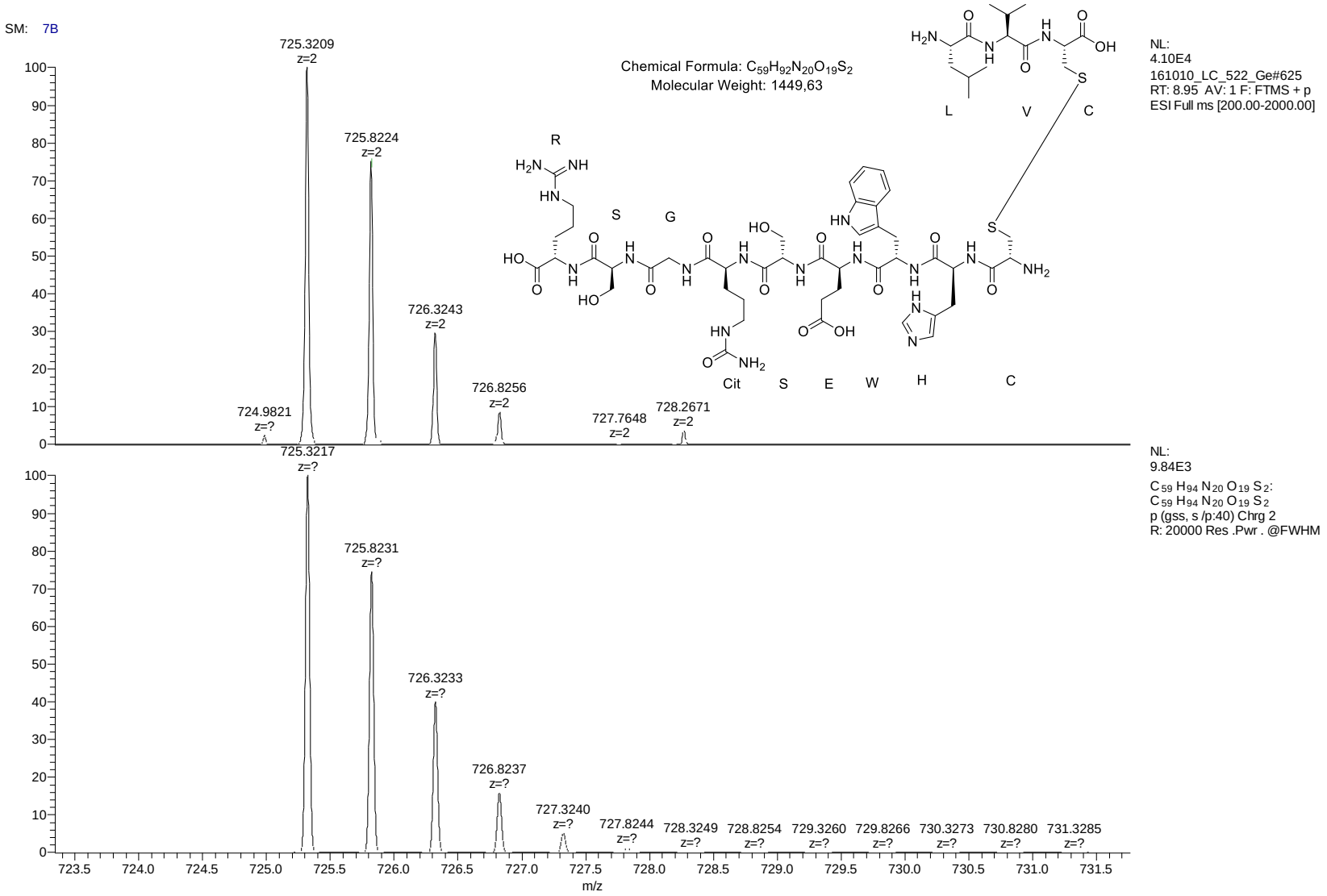

Figure S12. High resolution mass spectrum of the shown C1-C12/C1-C12 connected fragment of peptide dimer **2d**.

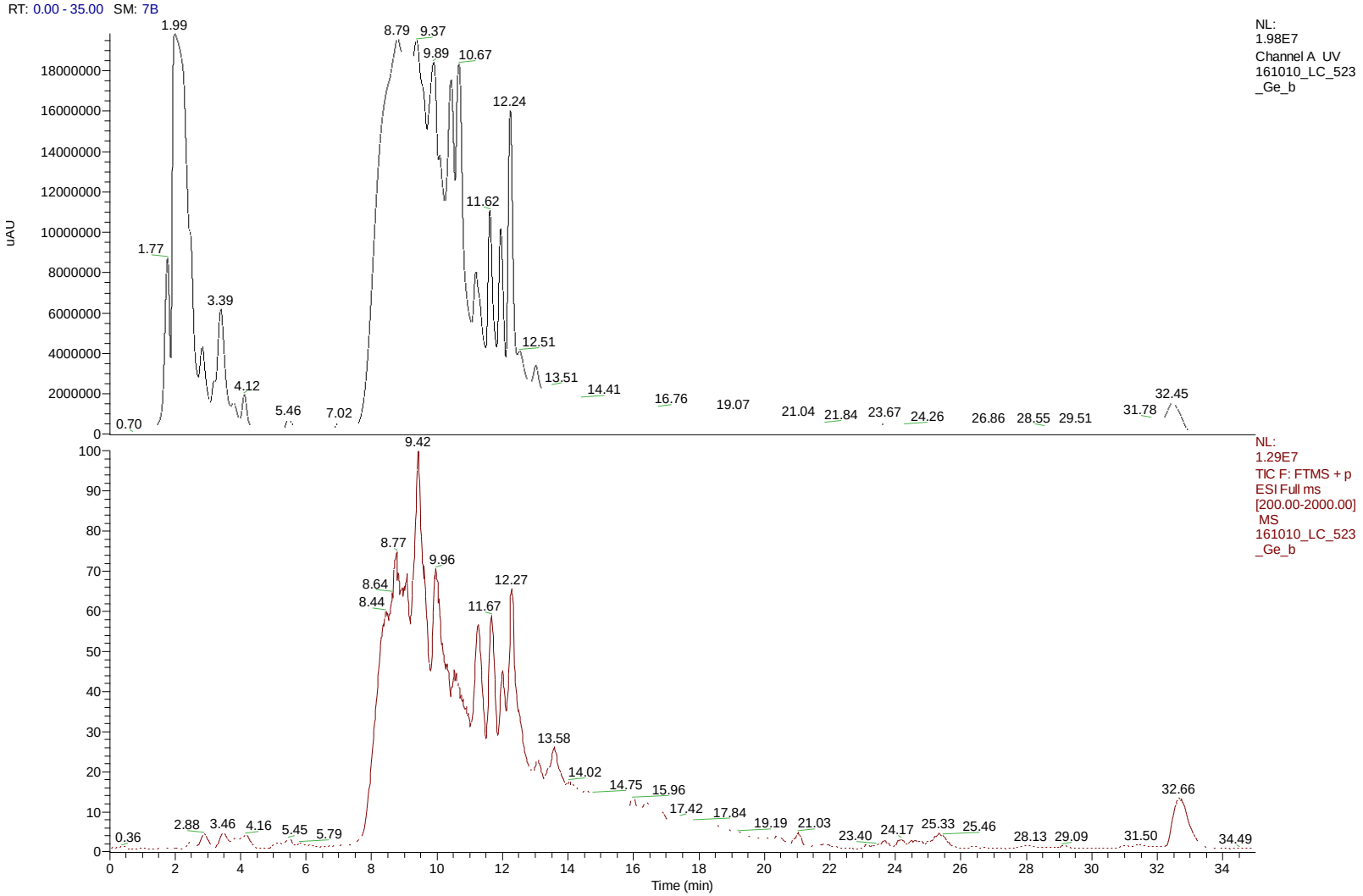

Figure S13. LC-MS chromatograms of peptide dimer **1d** after digestion with an excess of trypsin.

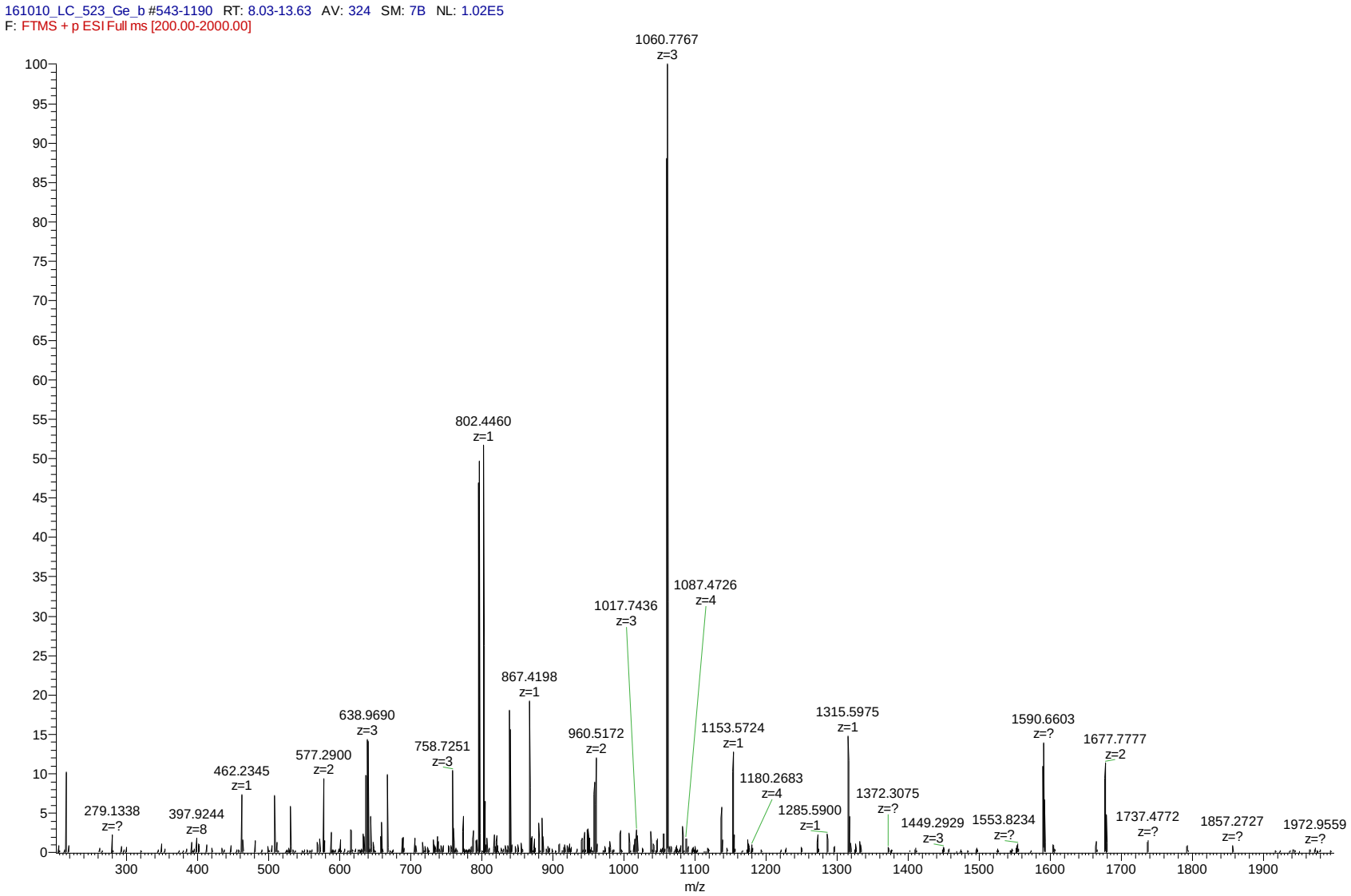

Figure S14. Mass spectrum of fragments from trypsin degradation of tetra-sulfide **1d**. The main peak (1060.7767, z=3) corresponds to the intact dimer structure.

Analytical HPLC

Analytical HPLC was done on a *Thermo Fisher Ultimate 3000 LC System* under the following conditions (if not indicated otherwise):

Column: ACE Ultracore 2.5 SuperC18, 150 mm x 2.1 mm id
Gradient: 10-40% B in 10 min (A: water + 0.1% TFA, B: acetonitrile + 0.85% TFA)
Flow rate: 0.45 mL/min

The concentration-dependent oxidation of peptide sequence **1** is shown in figure S15. Chromatograms of the different monomers and dimers are shown in figures S16-S23.

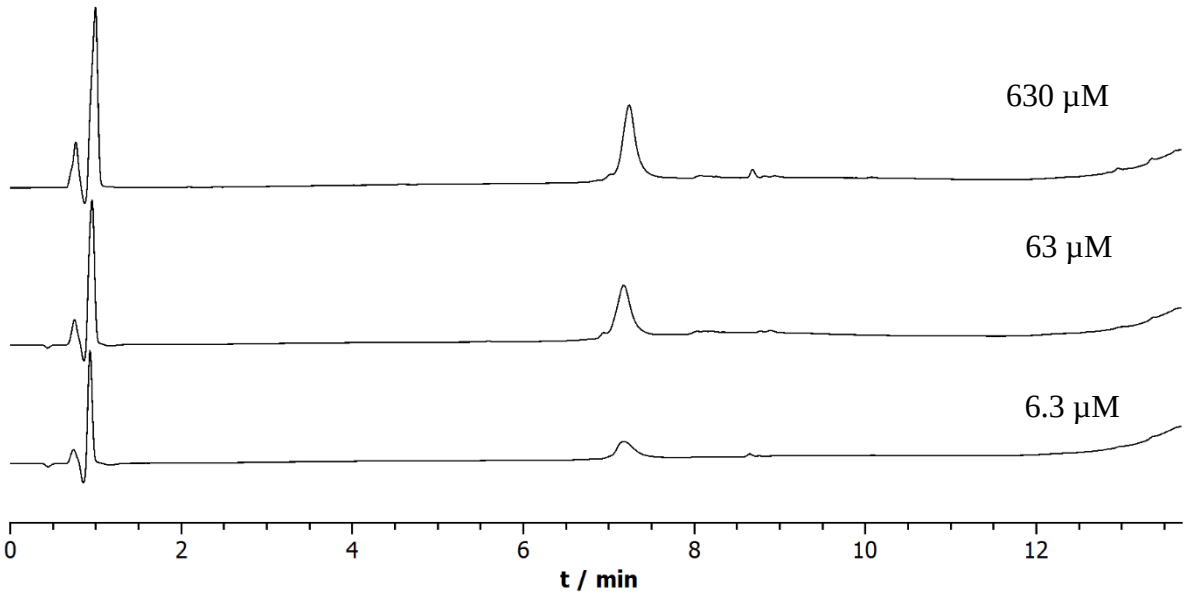

Figure S15. Chromatograms of crude peptide **1d** after air oxidation of the tetra-thiol precursor **1.** The concentration of the peptide in the $(NH_4)_2CO_3$ oxidation buffer is given at the right end of the respective elugram. The spectra prove, that only dimers are formed, even at minimal peptide concentrations.

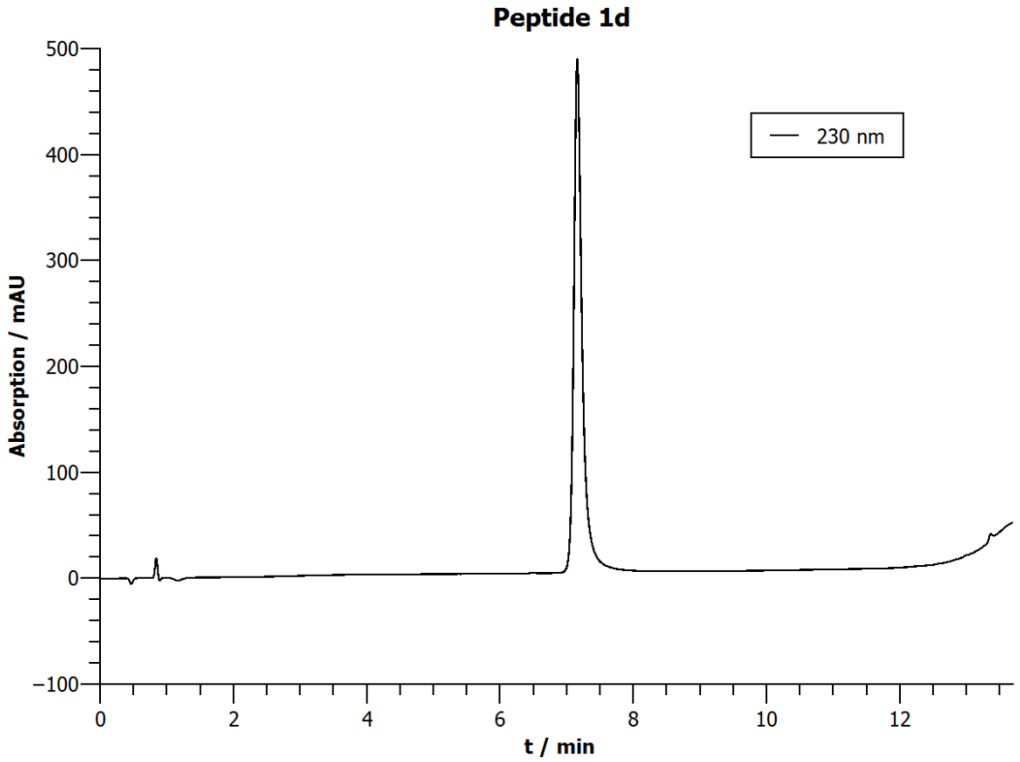

Figure S16. Chromatogram of peptide **1d**.

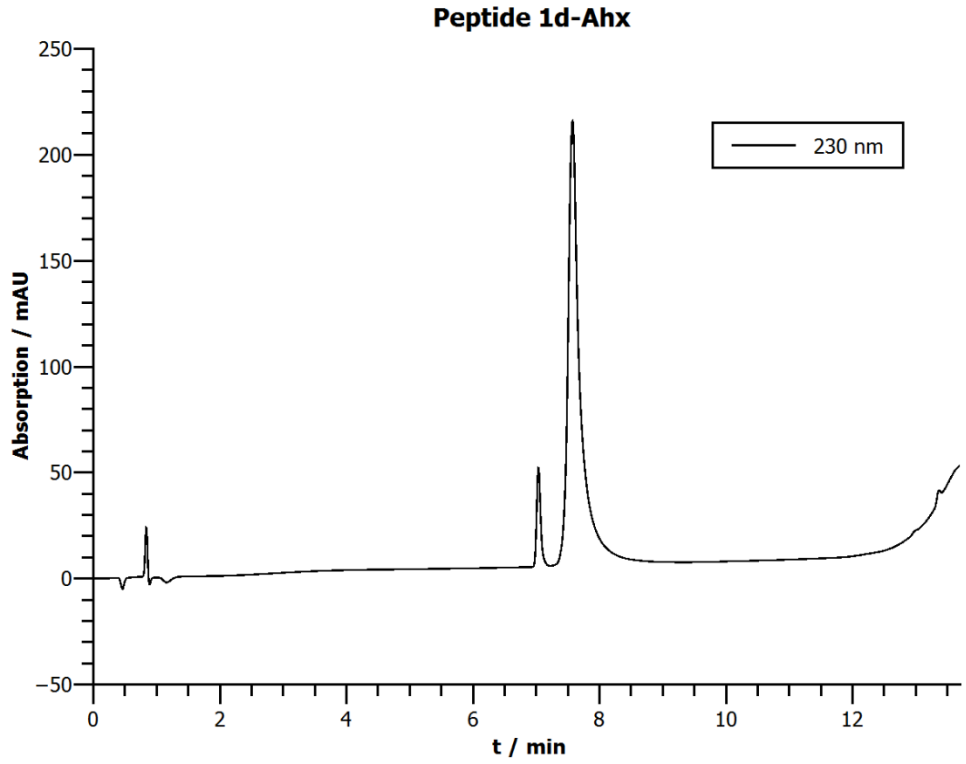

Figure S17. Chromatogram of peptide **1d-Ahx**. The minor impurity (~7 % as determined by integration of the signals) at t = 7.04 min cannot be assigned unambiguously, though the monomer mass could not be identified by HRMS.

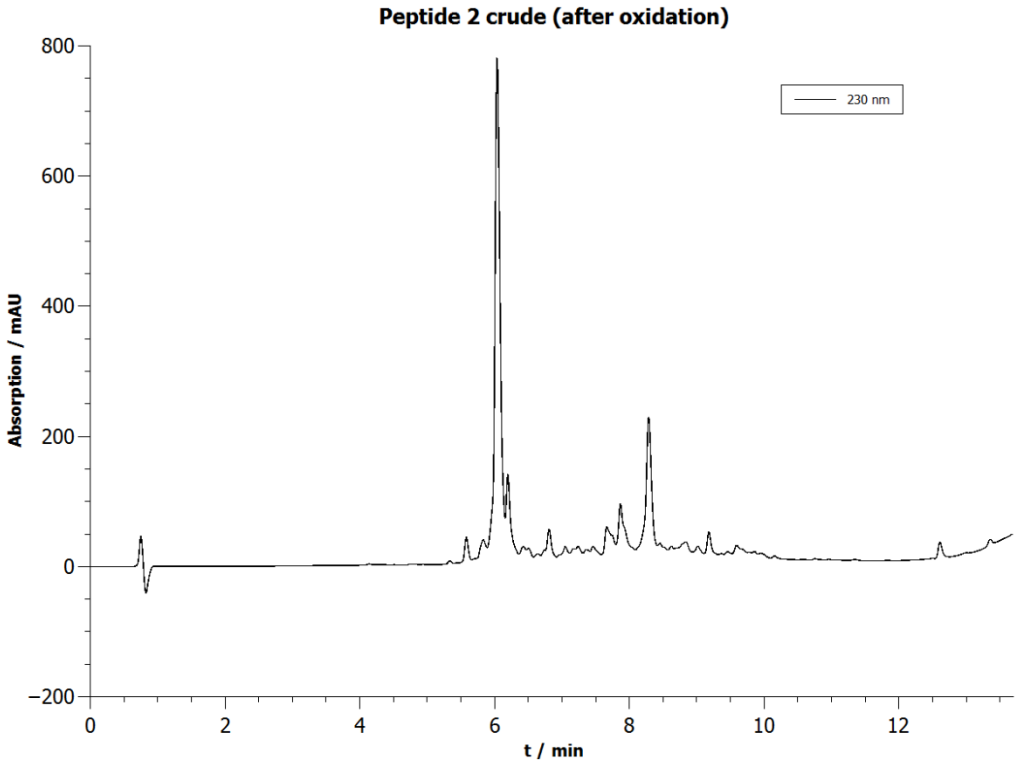

Figure S18. Chromatogram of crude peptide **2** after air oxidation.

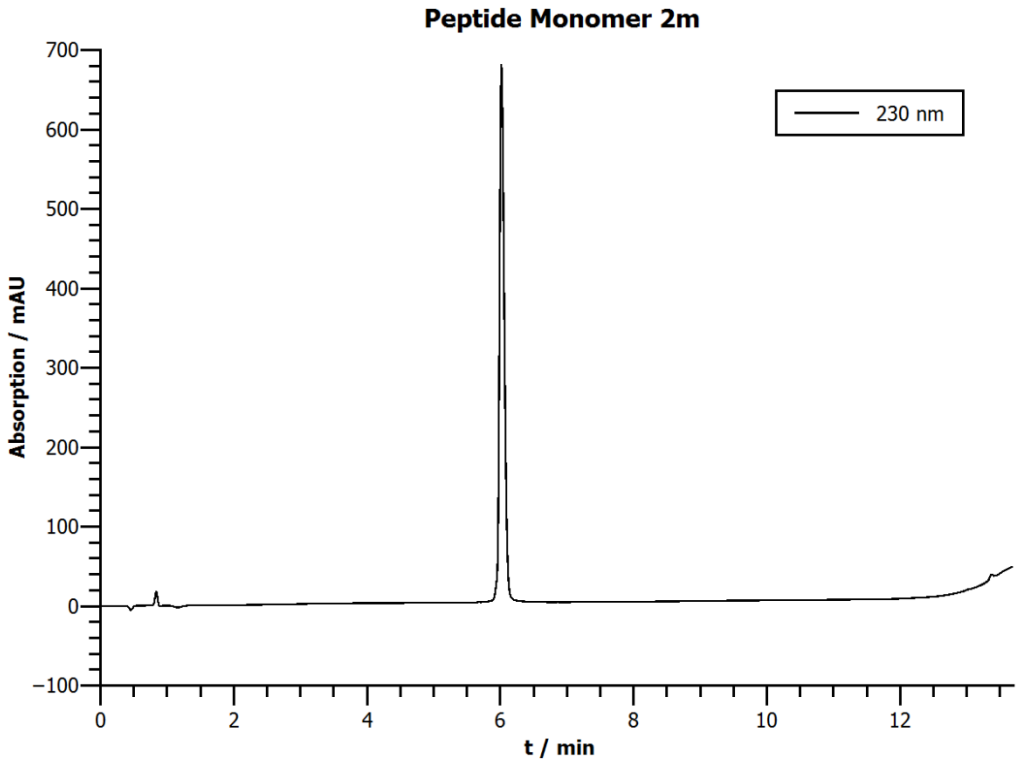

Figure S19. Chromatogram of peptide **2m**.

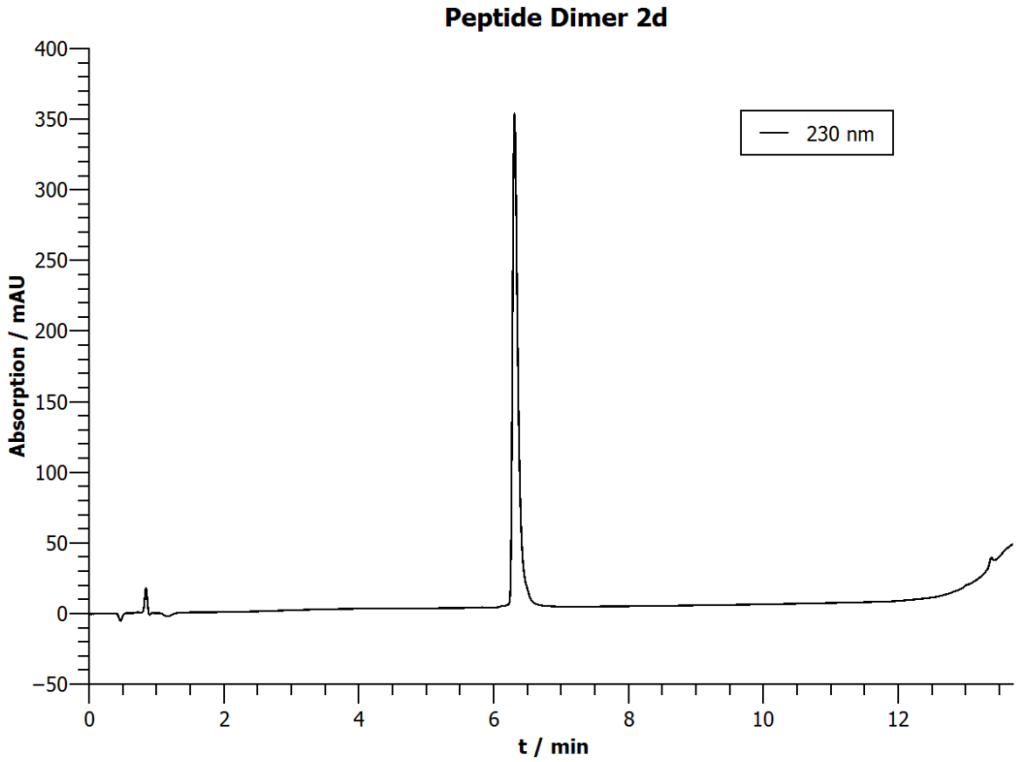

Figure S20. Chromatogram of peptide **2d**.

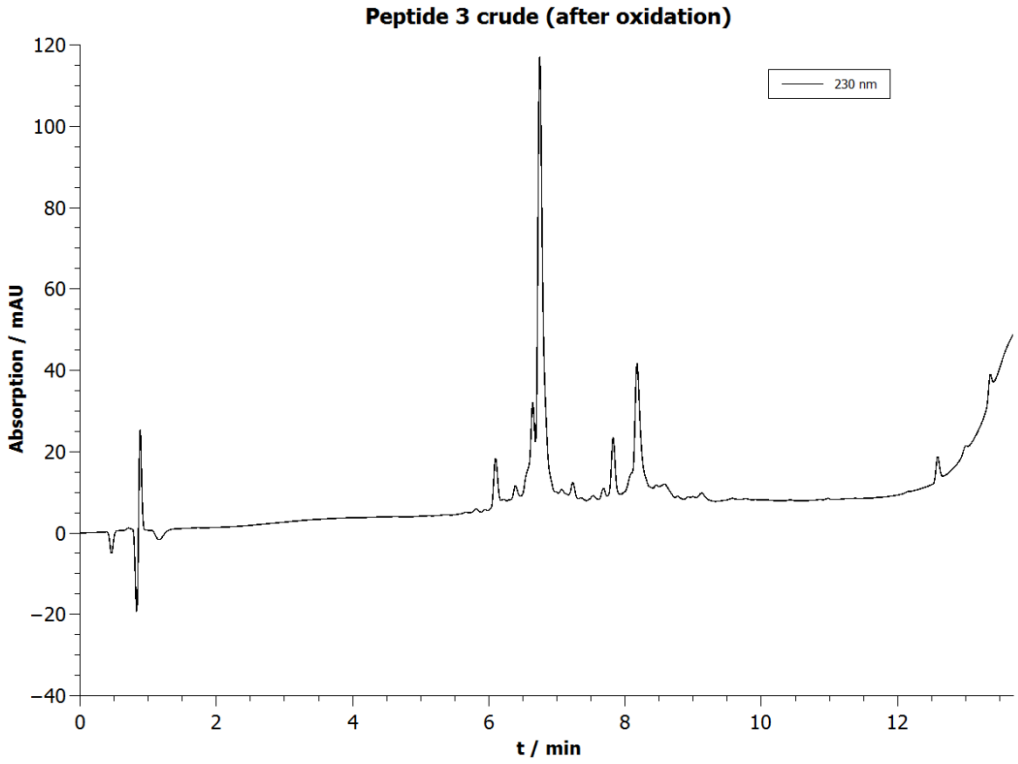

Figure S21. Chromatogram of crude peptide **3** after air oxidation.

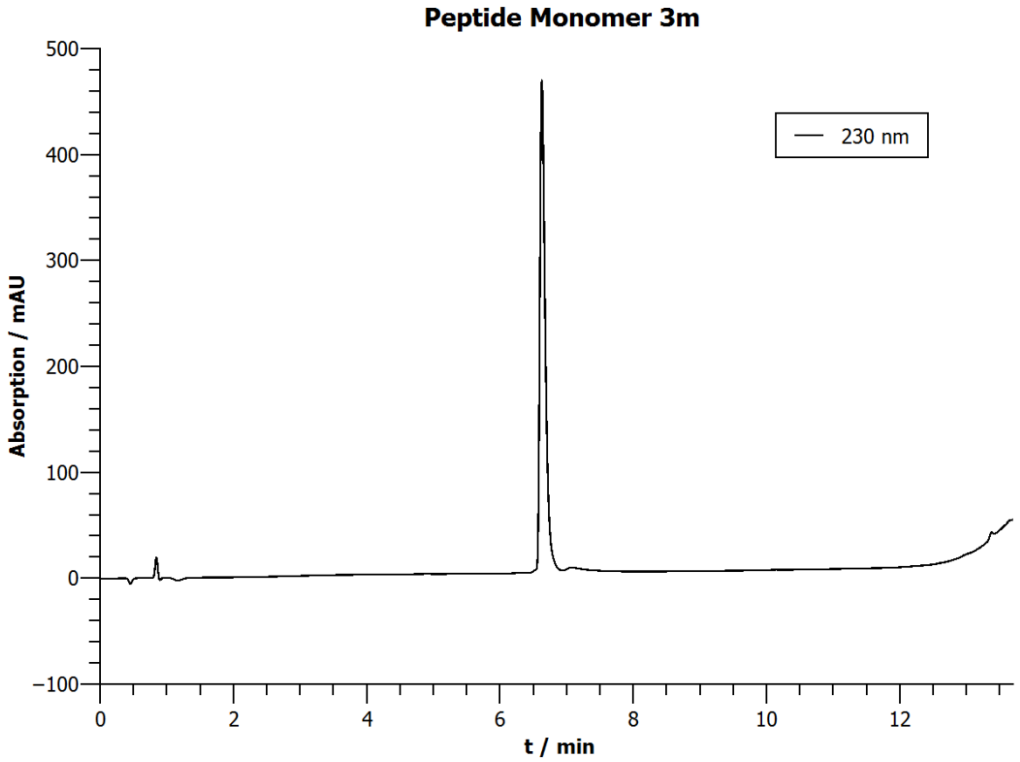

Figure S22. Chromatogram of peptide **3m-Ahx**.

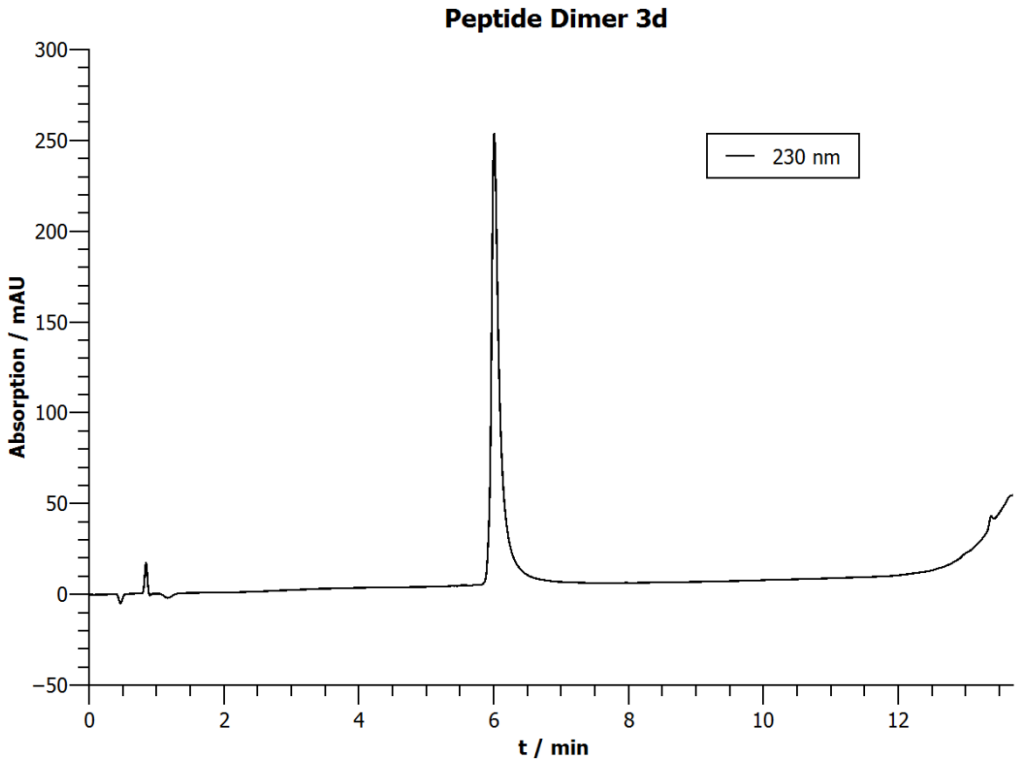

Figure S23. Chromatogram of peptide **3d**.

NMR measurement

One- and two-dimensional NMR spectra (1H, TOCSY, NOESY, ^{1}H-^{13}C-HSQC) were acquired on a *Bruker AV600* 600 MHz spectrometer at 280 K, 290 K or 300 K in 90% potassium phosphate buffer (50 mM, pH 3.0) and 10% D_2O using WATERGATE pulse sequence water suppression. NMR spectra were calibrated to the signal of the internal standard 3-(trimethylsilyl)-2,2,3,3-tetradeuteropropionic acid sodium salt (TSP-d_4) that was set to 0.00 ppm.

Tetra-disulfide 1d 300 K, pH = 3.0

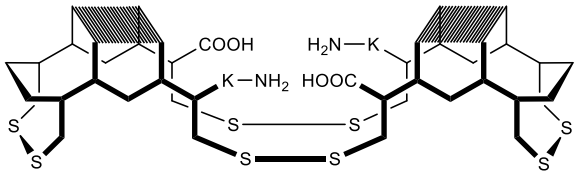

(H-K^{0}-C^{1}-H^{2}-W^{3}-E^{4}-C^{5}-Cit^{6}-G^{7}-C^{8}-R^{9}-L^{10}-V^{11}-C^{12}-OH)$_2$

Table S2. ^{1}H NMR signal assignment for tetra-disulfide **1d**.

Amino Acid	δ(α) / ppm	δ(β) / ppm	δ(γ) / ppm	δ(other) / ppm	δ(NH) / ppm
Lys^{0}	4.09	1.93	1.47	δ: 1.73, ε: 3.01 ζ(NH_3^+): 7.60	-
Cys^{1}	5.26	3.04, 2.49	-	-	8.48
His^{2}	4.97	3.29	-	aromatic: δ^2: 7.06, ε^1: 8.53	8.90
Trp^{3}	4.92	2.93, 2.77	-	aromatic: 2: 7.00, 1(NH): 10.51, 4: 6.52, 7: 7.54, 5: 6.32, 6: 7.30	8.48
Glu^{4}	5.61	1.99, 1.87	2.36, 2.31	-	9.37
Cys^{5}	5.61	3.00	-	-	9.33
Cit^{6}	4.85	1.89	1.67	δ: 3.20 ε(NH): n/a	8.63
Gly^{7}	4.33, 3.84	-	-	-	n/a
Cys^{8}	5.26	2.14, 0.10	-	-	6.21
Arg^{9}	4.47	1.71, 1.60	1.40	δ: 3.11 ε(NH): 7.07	8.83
Leu^{10}	3.47	1.20, -0.03	0.70	δ: 0.40, -0.32	8.52
Val^{11}	3.99	1.29	0.79, 0.64	-	8.71
Cys^{12}	4.70	3.06, 2.84	-	-	8.35

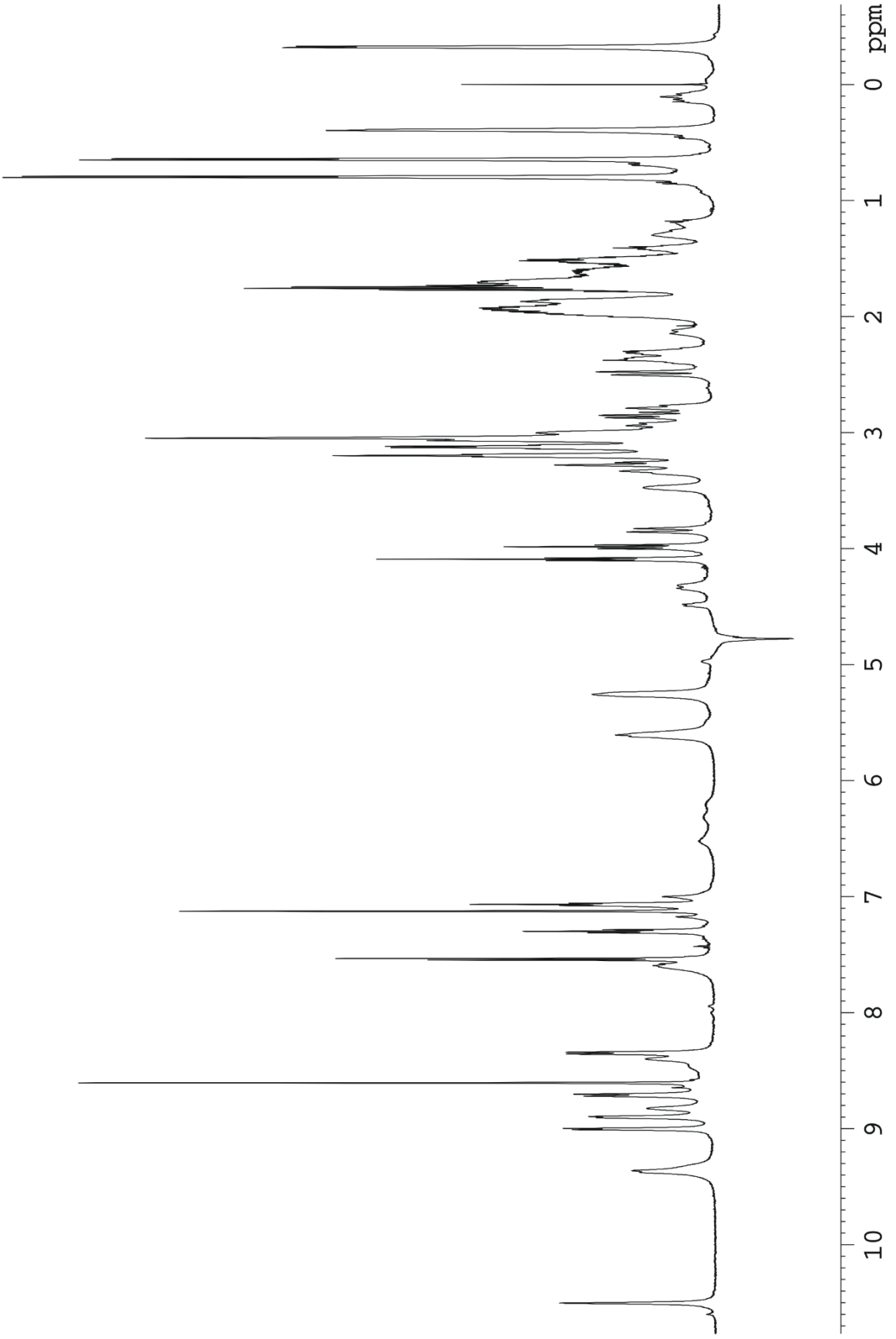

Figure S24. ^{1}H NMR spectrum of tetra-disulfide **1d** (600 MHz, 300 K, 50 mM potassium phosphate buffer (pH 3.0)/D_2O 9:1).

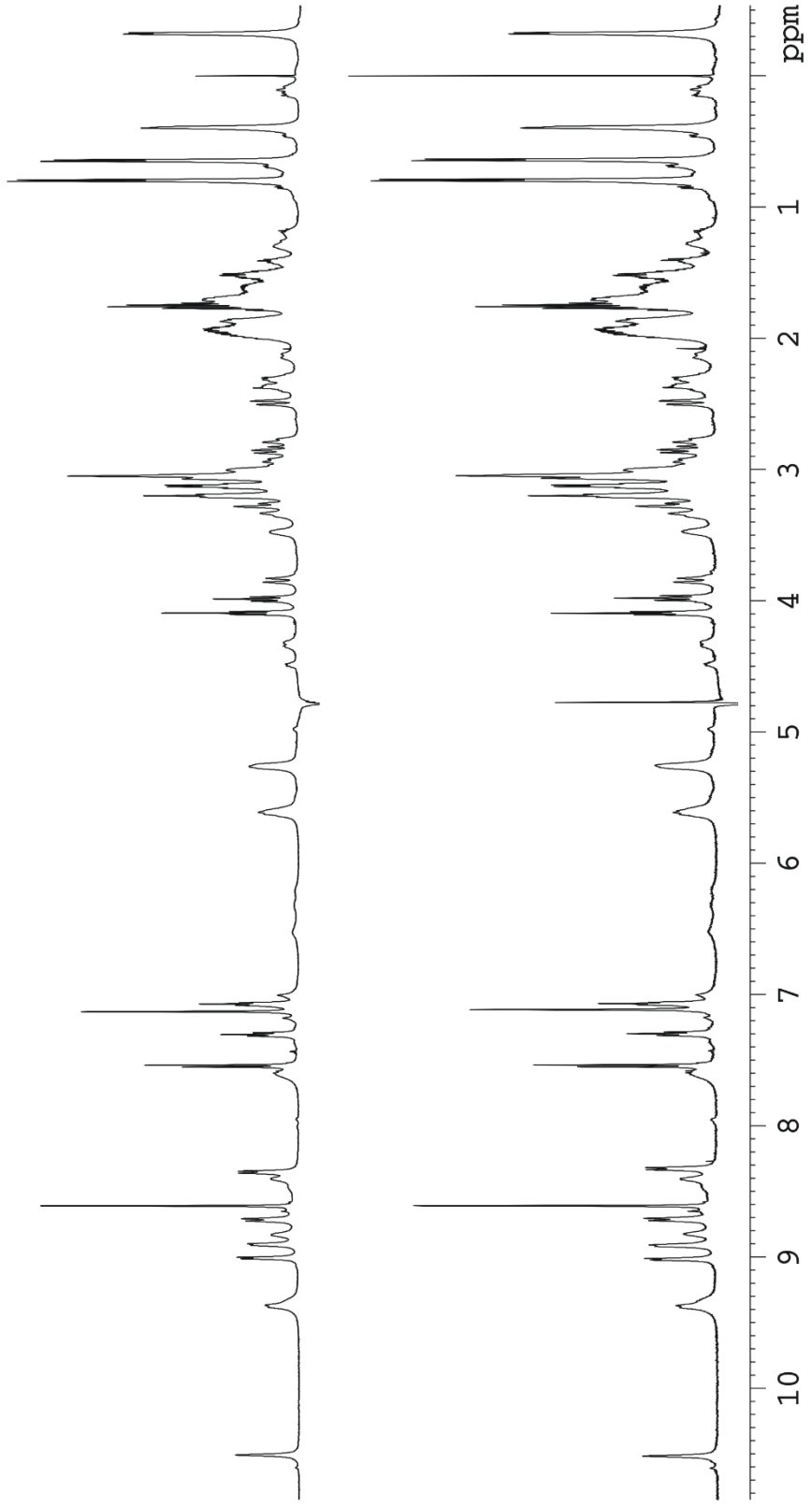

Figure S25. ^{1}H NMR spectrum of tetra-disulfide **1d** (600 MHz, 300 K, 50 mM potassium phosphate buffer (pH 3.0)/D_2O 9:1) with different peptide concentrations. Left: 3.00 mg/mL / 1.57 mM; Right: 1.50 mg/mL / 0.79 mM.

Tetra-disulfide 1d-Ahx 300 K, pH = 3.0

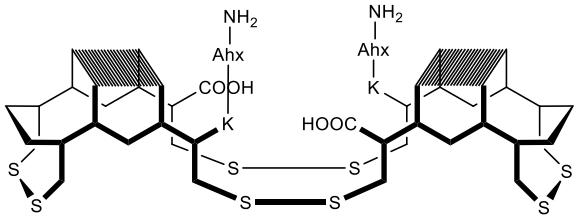

(H-K^{-1}-Ahx^{0}-C^{1}-H^{2}-W^{3}-E^{4}-C^{5}-Cit^{6}-G^{7}-C^{8}-R^{9}-L^{10}-V^{11}-C^{12}-OH)$_2$

Table S3. ^{1}H NMR signal assignment for tetra-disulfide **1d-Ahx**.

Amino Acid	δ(α) / ppm	δ(β) / ppm	δ(γ) / ppm	δ(other) / ppm	δ(NH) / ppm
Lys^{-1}	3.93	1.90	1.47	δ: 1.71, ε: 3.01 ζ(NH_3^+): 7.57	n/a
Ahx^{0}	2.34	1.56	1.38	δ: 1.64, ε: 3.24	8.44
Cys^{1}	5.19	3.03, 2.48	-	-	8.44
His^{2}	5.00	3.32	-	aromatic: δ^2: 7.13, ε^1: 8.58	8.85
Trp^{3}	4.92	2.92, 2.78	-	aromatic: 2: 7.02, 1(NH): 10.50, 4: 6.51, 7: 7.54, 5: 6.32, 6: 7.30	8.48
Glu^{4}	5.62	1.93, 1.87	2.37, 2.33	-	9.36
Cys^{5}	5.62	3.00	-	-	9.36
Cit^{6}	4.89	1.89	1.67	δ: 3.20 ε(NH): n/a	8.63
Gly^{7}	4.33, 3.84	-	-	-	n/a
Cys^{8}	5.26	2.14, 0.10	-	-	6.21
Arg^{9}	4.47	1.71, 1.60	1.40	δ: 3.11 ε(NH): 7.07	8.83
Leu^{10}	3.47	1.19, -0.06	0.70	δ: 0.40, -0.33	8.41
Val^{11}	3.99	1.30	0.81, 0.65	-	8.74
Cys^{12}	4.76	3.06, 2.85	-	-	8.44

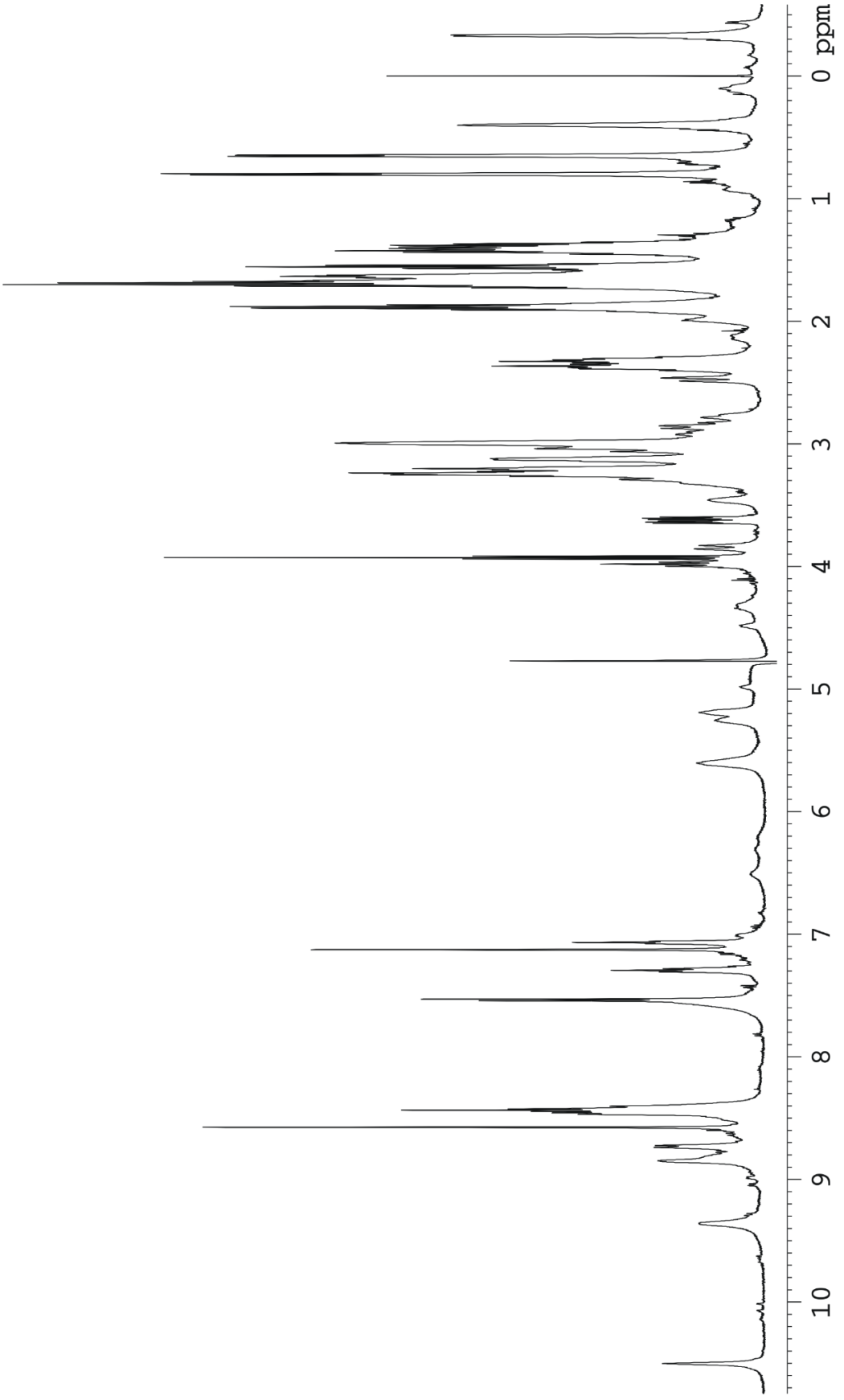

Figure S26. ^{1}H NMR spectrum of tetra-disulfide **1d-Ahx** (600 MHz, 300 K, 50 mM potassium phosphate buffer (pH 3.0)/D_2O 9:1).

Epitope monomer 2m 300 K, pH = 3.0

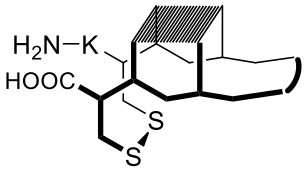

H-K^{0}-C^{1}-H^{2}-W^{3}-E^{4}-S^{5}-Cit^{6}-G^{7}-S^{8}-R^{9}-L^{10}-V^{11}-C^{12}-OH

Table S4. ^{1}H NMR signal assignment for monomer **2m**.

Amino Acid	δ(α) / ppm	δ(β) / ppm	δ(γ) / ppm	δ(other) / ppm	δ(NH) / ppm
Lys^{0}	4.09	1.94	1.47	δ: 1.73, ε: 3.02	-
Cys^{1}	5.20	3.06, 2.61	-	-	8.98
His^{2}	4.89	3.24	-	aromatic: δ^{2}: 7.27, ε^{1}: 8.63	9.07
Trp^{3}	4.79	3.12	-	aromatic: 2: 7.16, 1(NH): 10.11, 4: 7.31, 7: 7.43, 5: 6.97, 6: 7.15	8.86
Glu^{4}	4.63	2.11, 1.81	2.37	-	8.78
Ser^{5}	4.14	3.94	-	-	8.56
Cit^{6}	4.14	1.79	1.49	δ: 3.09 ε(NH): n/a	8.56
Gly^{7}	3.91, 3,70	-	-	-	8.15
Ser^{8}	4.09	3.98	-	-	7.82
Arg^{9}	4.47	1.67, 1.60	1.38	δ: 3.08 ε(NH): 7.05	7.55
Leu^{10}	4.29	1.53, 1.09	1.27	δ: 0.69, 0.41	8.43
Val^{11}	4.17	1.65	0.88, 0.74	-	8.59
Cys^{12}	4.73	3.11, 2.91	-	-	8.45

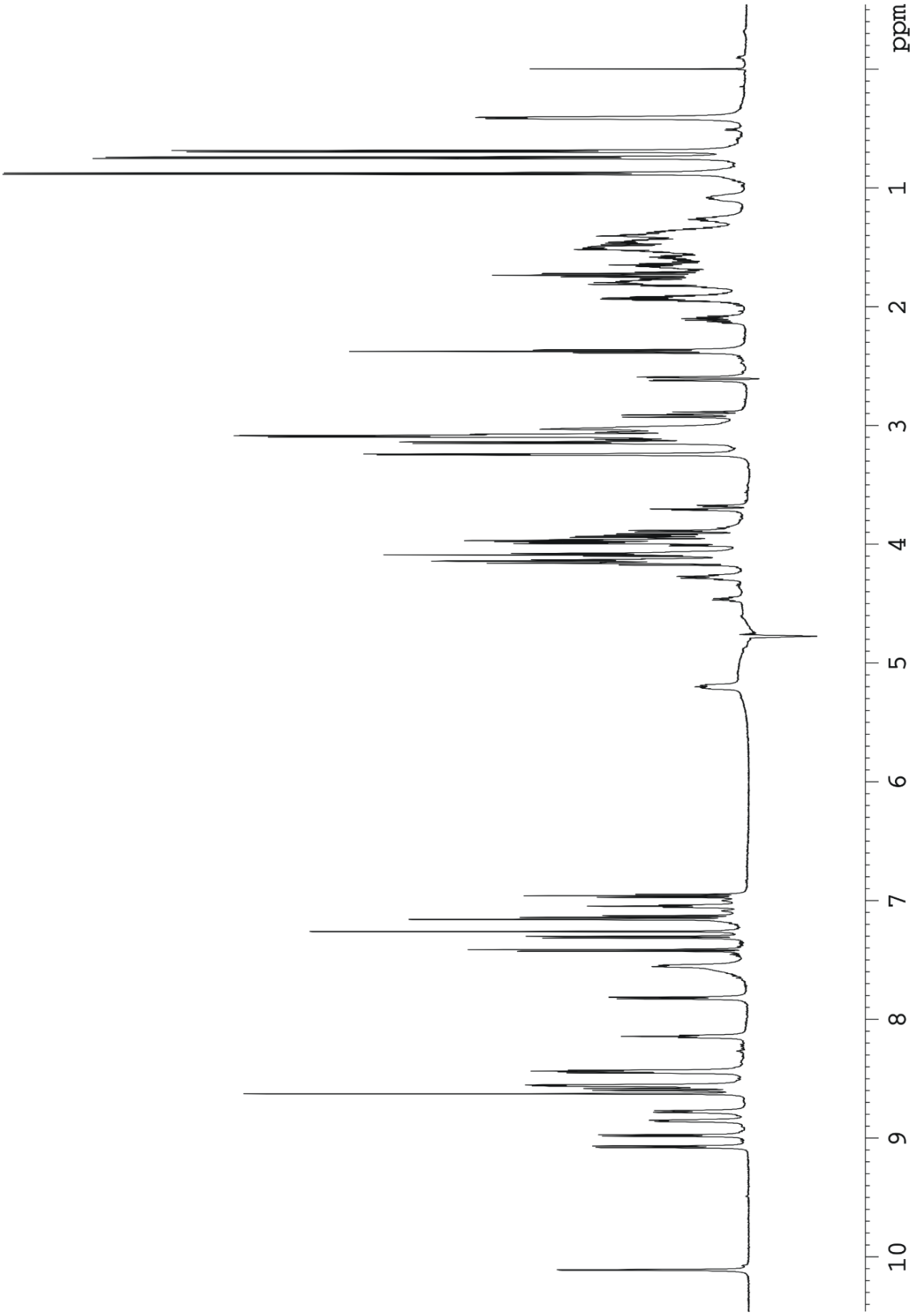

Figure S27. ^{1}H NMR spectrum of epitope monomer **2m** (600 MHz, 300 K, 50 mM potassium phosphate buffer (pH 3.0)/D_2O 9:1).

Epitope dimer 2d 300 K, pH = 3.0

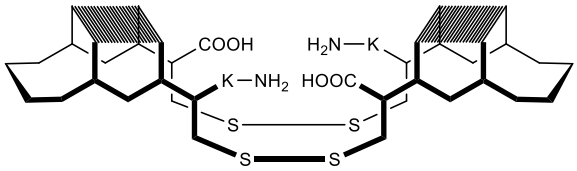

$\overline{(H\text{-}K^{0}\text{-}C^{1}}\text{-}H^{2}\text{-}W^{3}\text{-}E^{4}\text{-}S^{5}\text{-}Cit^{6}\text{-}G^{7}\text{-}S^{8}\text{-}R^{9}\text{-}L^{10}\text{-}V^{11}\text{-}\overline{C^{12}\text{-}OH)}_{2}$

Table S5. ^{1}H NMR signal assignment for dimer **2d**.

Amino Acid	δ(α) / ppm	δ(β) / ppm	δ(γ) / ppm	δ(other) / ppm	δ(NH) / ppm
Lys^{0}	4.09	1.93	1.47	δ: 1.73, ε: 3.01 ζ(NH_3^+): 7.60	-
Cys^{1}	5.28	3.03, 2.45	-	-	8.92
His^{2}	4.87	3.24	-	aromatic: δ^2: 7.28, ε^1: 8.61	8.94
Trp^{3}	4.87	3.09	-	aromatic: 2: 7.27, 1(NH): 10.11, 4: 7.20, 7: 7.47, 5: 6.96, 6: 7.21	8.94
Glu^{4}	4.88	2.16, 1.87	2.43	-	9.43
Ser^{5}	4.70	4.03, 3.84	-	-	8.84
Cit^{6}	4.36	1.89	1.40	δ: 3.07, 2.97 ε(NH): n/a	8.78
Gly^{7}	4.38, 3,87	-	-	-	8.44
Ser^{8}	5.37	3.87, 3.67	-	-	8.54
Arg^{9}	4.89	1.76	1.48	δ: 3.12 ε(NH): 7.11	9.21
Leu^{10}	3.72	1.26, 0.06	0.74	δ: 0.41, -0.31	8.52
Val^{11}	4.09	1.57	0.85, 0.71	-	8.69
Cys^{12}	4.98	3.15, 2.92	-	-	8.83

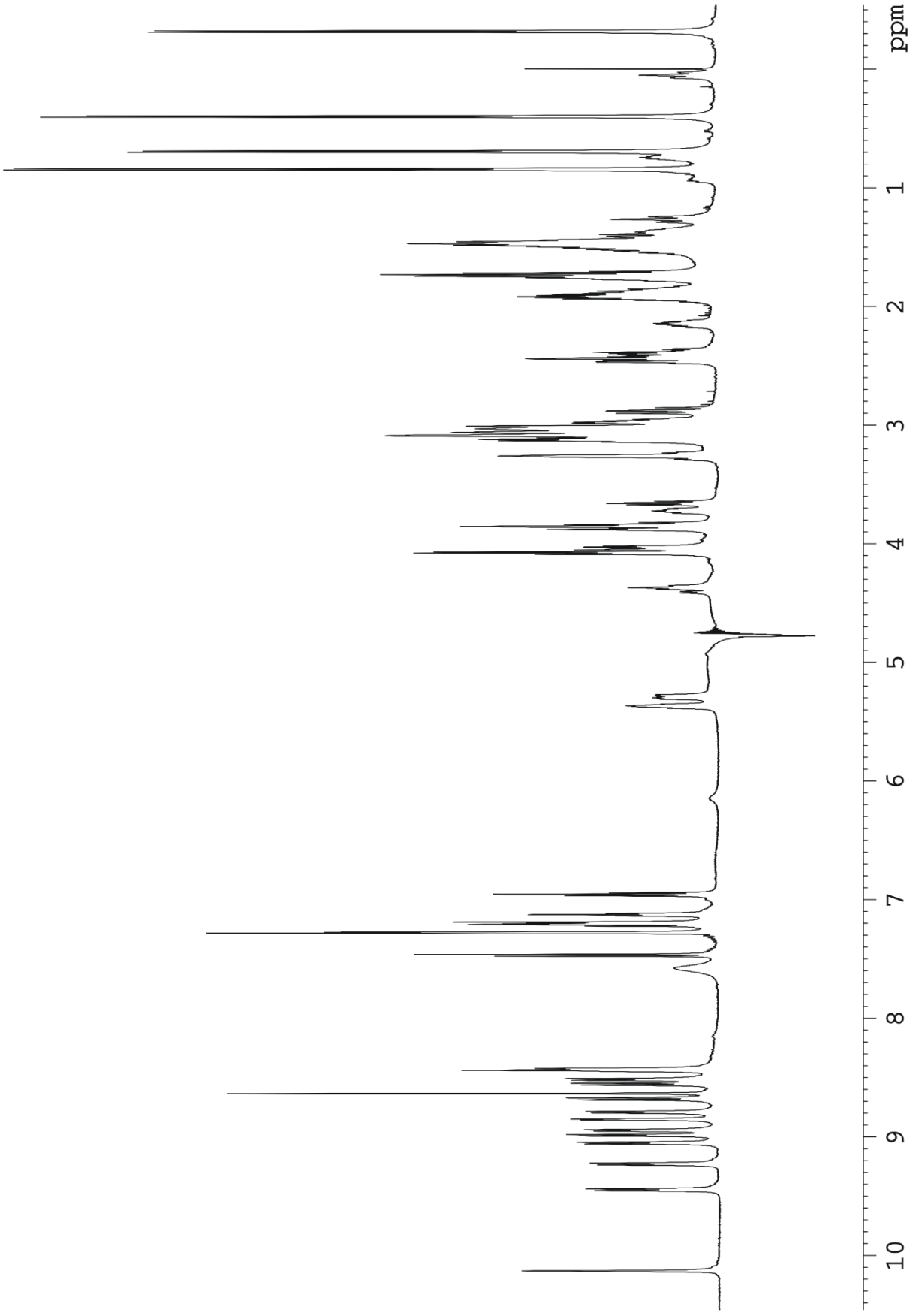

Figure S28. ^{1}H NMR spectrum of epitope dimer **2d** (600 MHz, 300 K, 50 mM potassium phosphate buffer (pH 3.0)/D_2O 9:1).

Epitope monomer 3m-Ahx 300 K, pH = 3.0

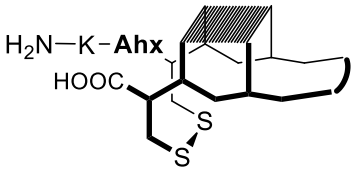

H-K^{-1}-Ahx^{0}-C^{1}-H^{2}-W^{3}-E^{4}-T^{5}-Cit^{6}-G^{7}-R^{8}-R^{9}-L^{10}-V^{11}-C^{12}-OH

Table S6. ^{1}H NMR signal assignment for monomer **3m-Ahx**.

Amino Acid	δ(α) / ppm	δ(β) / ppm	δ(γ) / ppm	δ(other) / ppm	δ(NH) / ppm
Lys^{-1}	3.93	1.89	1.43	δ: 1.70, ε: 2.99 ζ(NH_3^+): 7.57	-
Ahx^{0}	2.33	1.56	1.36	δ: 1.64, ε: 3.24	8.43
Cys^{1}	5.13	3.02, 2.59		-	8.42
His^{2}	4.87	3.24		aromatic: δ^2: 7.22, ε^1: 8.60	8.99
Trp^{3}	4.67	3.14		aromatic: 2: 7.14, 1(NH): 10.15, 4: 7.32, 7: 7.36, 5: 6.99, 6: 7.12	8.84
Glu^{4}	4.63	2.10, 1.86	2.40	-	8.66
Thr^{5}	4.21	4.02	1.33	-	8.38
Cit^{6}	4.17	1.77	1.52, 1.46	δ: 3.09 ε(NH): n/a	8.52
Gly^{7}	3.78	-	-	-	8.00
Arg^{8}	3.79	1.87	1.66	δ: 3.24 ε(NH): 7.19	7.82
Arg^{9}	4.41	1.68, 1.59	1.33	δ: 3.08 ε(NH): 7.04	7.30
Leu^{10}	4.33	1.55, 1.16	1.31	δ: 0.72, 0.49	8.44
Val^{11}	4.17	1.66	0.87, 0.75	-	8.64
Cys^{12}	4.73	3.10, 2.92		-	8.48

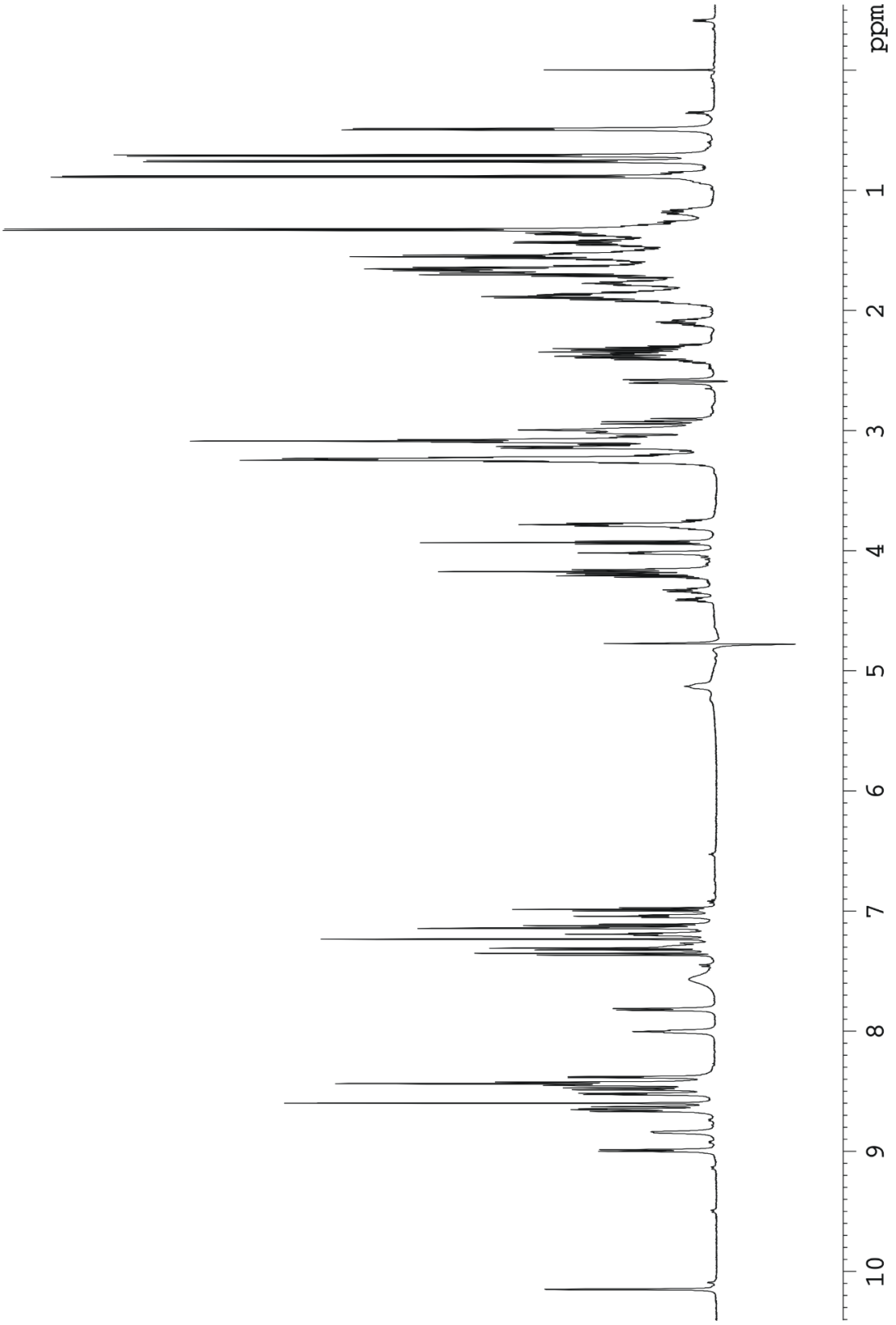

Figure S29. ^{1}H NMR spectrum of epitope monomer **3m-Ahx** (600 MHz, 300 K, 50 mM potassium phosphate buffer (pH 3.0)/D_2O 9:1).

Epitope dimer 3d 300 K, pH = 3.0

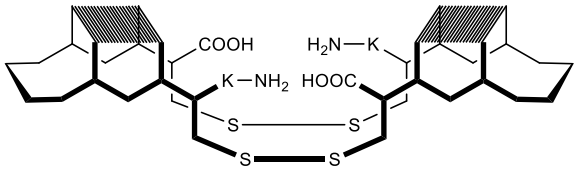

(H-K^{0}-C^{1}-H^{2}-W^{3}-E^{4}-T^{5}-Cit^{6}-G^{7}-R^{8}-R^{9}-L^{10}-V^{11}-C^{12}-OH)$_2$

Table S7. ^{1}H NMR signal assignment for dimer **3d**.

Amino Acid	δ(α) / ppm	δ(β) / ppm	δ(γ) / ppm	δ(other) / ppm	δ(NH) / ppm
Lys^{0}	4.07	1.92	1.47	δ: 1.73, ε: 3.02 ζ(NH_3^+): 7.57	-
Cys^{1}	5.29	2.97, 2.43		-	9.00
His^{2}	4.83	3.26		aromatic: δ^2: 7.26, ε^1: 8.64	9.06
Trp^{3}	4.96	3.10, 2.99		aromatic: 2: 7.27, 1(NH): 10.09, 4: 7.16, 7: 7.45, 5: 6.92, 6: 7.20	8.93
Glu^{4}	4.93	2.20, 1.91	2.44	-	9.51
Thr^{5}	4.54	4.25	1.24	-	8.74
Cit^{6}	4.17	1.85, 1.56	1.45	δ: 3.05 ε(NH): n/a	8.42
Gly^{7}	4.11, 4.07	-	-	-	8.36
Arg^{8}	5.10	1.85, 1.71	1.53	δ: 2.80, 2.63 ε(NH): 6.53	8.51
Arg^{9}	4.89	1.75	1.50	δ: 3.13 ε(NH): 7.04	9.14
Leu^{10}	3.75	1.23, 0.09	1.26	δ: 0.35, -0.41	8.61
Val^{11}	4.07	1.47	0.85, 0.70	-	8.66
Cys^{12}	4.73	3.05, 2.86		-	8.39

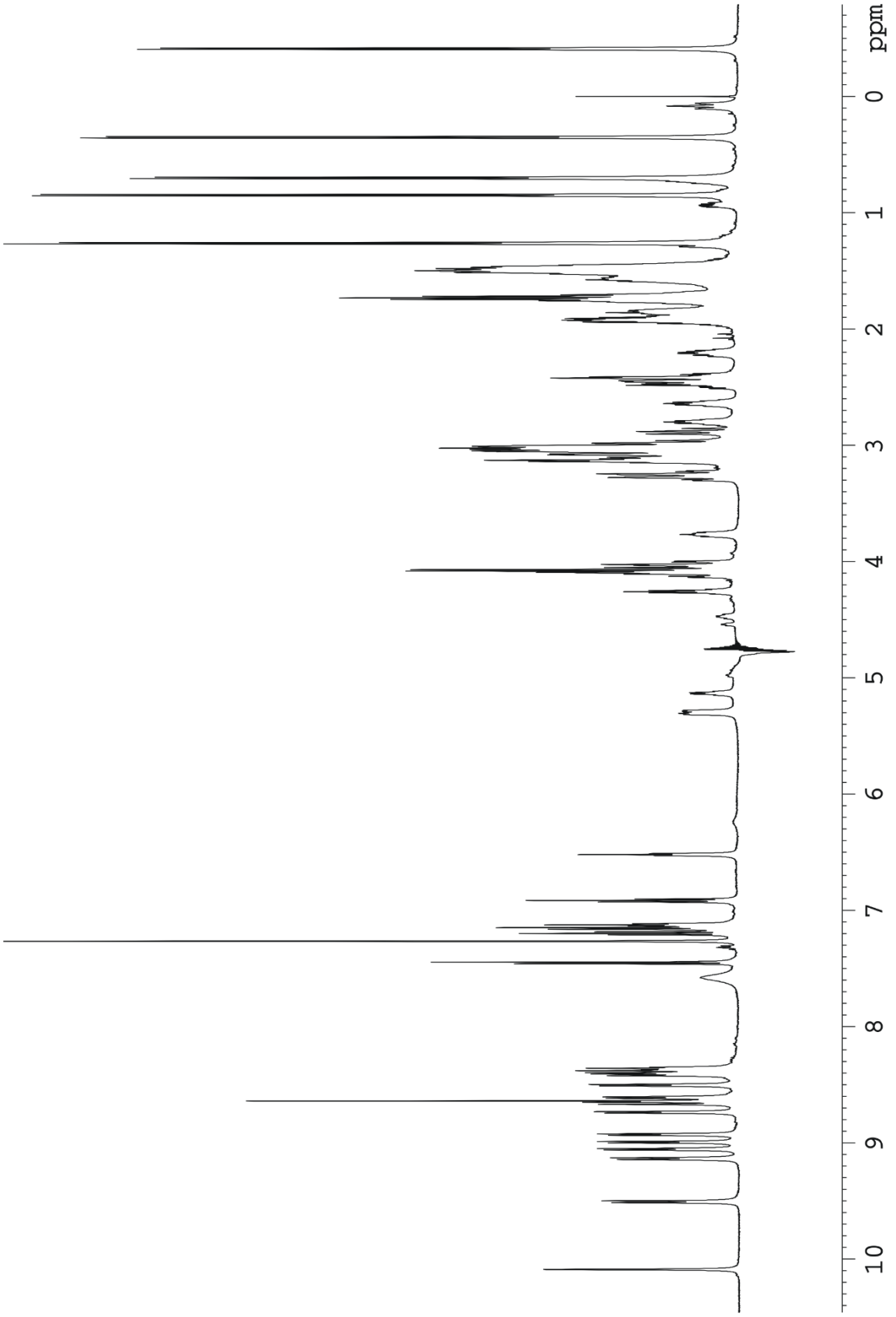

Figure S30. ^{1}H NMR spectrum of epitope dimer **3d** (600 MHz, 300 K, 50 mM potassium phosphate buffer (pH 3.0)/D_2O 9:1).

Temperature Gradients

^{1}H NMR spectra were measured at 280 K, 290 K and 300 K. For tetra-disulfide **1d**, ^{1}H NMR spectra were additionally measured at 310 K, 320 K and 330 K (depicted in figure S31). The change of shift for every NH signal was determined as ppb/K. Amide protons in hydrogen bonds are less dependent on temperature than those exposed to solvent. A large dispersion of those values and the typical alternating higher and lower dependencies for a rigid hairpin motif prove the integrity of the structure. Figure S32-S36 show measured values for monomers as well as dimers schematically.

Figure S37 shows the Leu-Hδ region for tetra-disulfide **1d**. The dispersion and highfield shift of these proton signals are a sign for an intact hydrophobic cluster (major stabilising element, built up between C1-E4 and R9-C12).

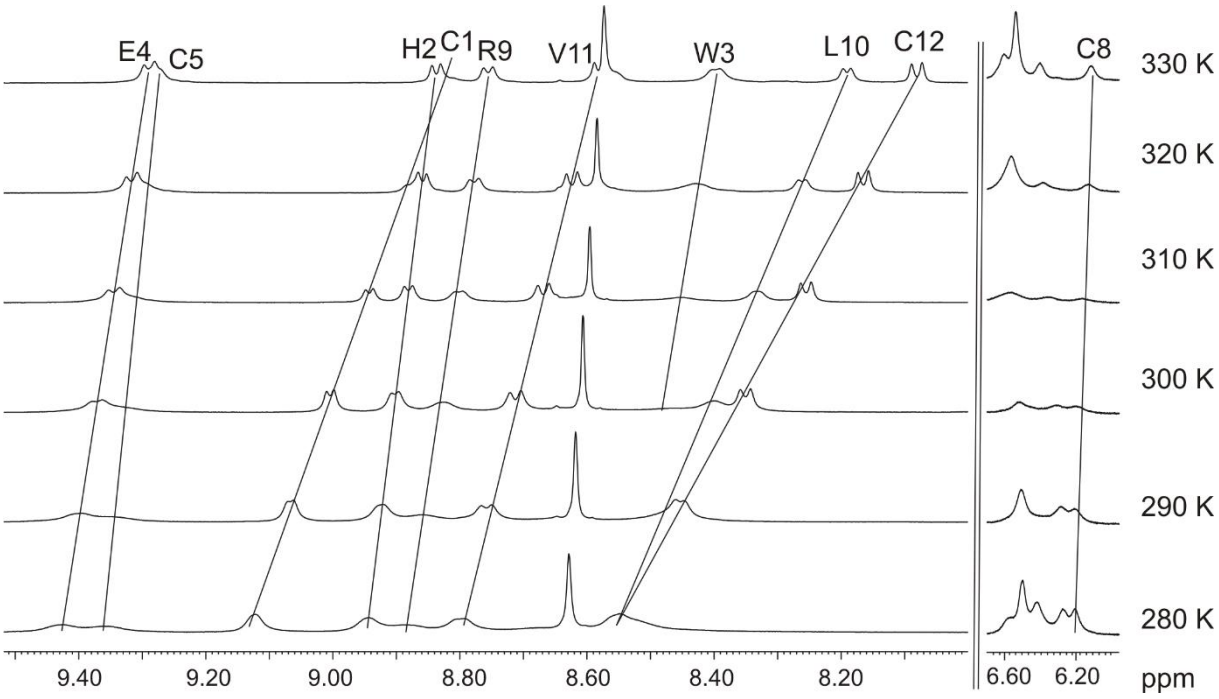

Figure S31. Temperature dependent ^{1}H NMR measurements of tetra-disulfide **1d**. The amide region is depicted and the lines indicate the temperature dependent shift of the amide signals (600 MHz, 50 mM potassium phosphate buffer (pH 3.0)/D_2O 9:1).

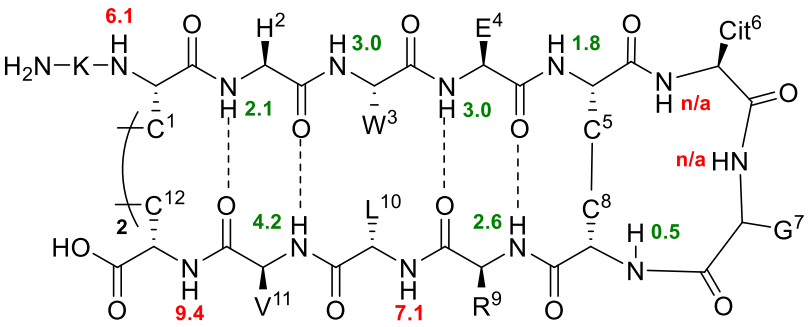

Figure S32. Temperature gradients of amide protons for tetra-disulfide **1d**.

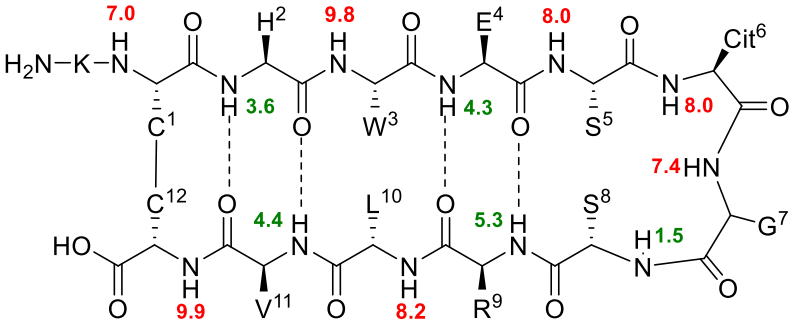

Figure S33. Temperature gradients of amide protons for monomer **2m**.

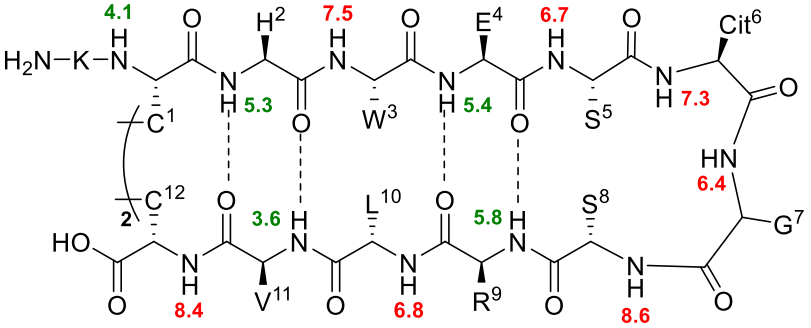

Figure S34. Temperature gradients of amide protons for dimer **2d**.

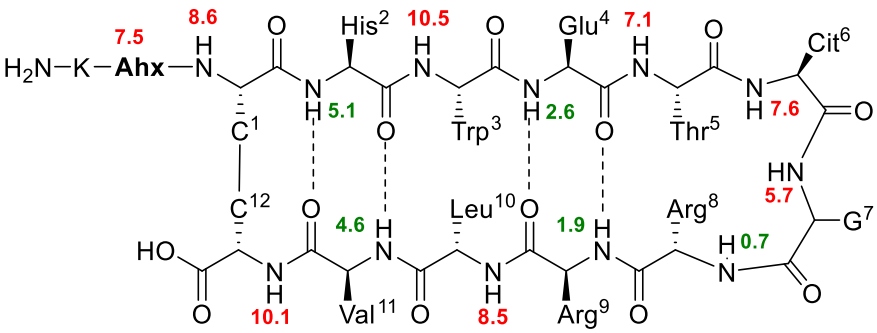

Figure S35. Temperature gradients of amide protons for monomer **3m-Ahx**.

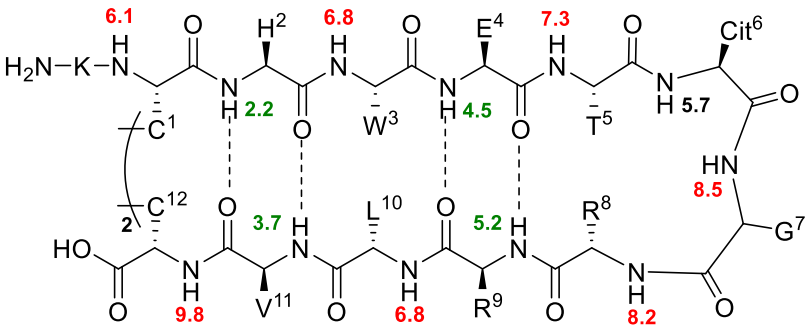

Figure S36. Temperature gradients of amide protons for dimer **3d**.

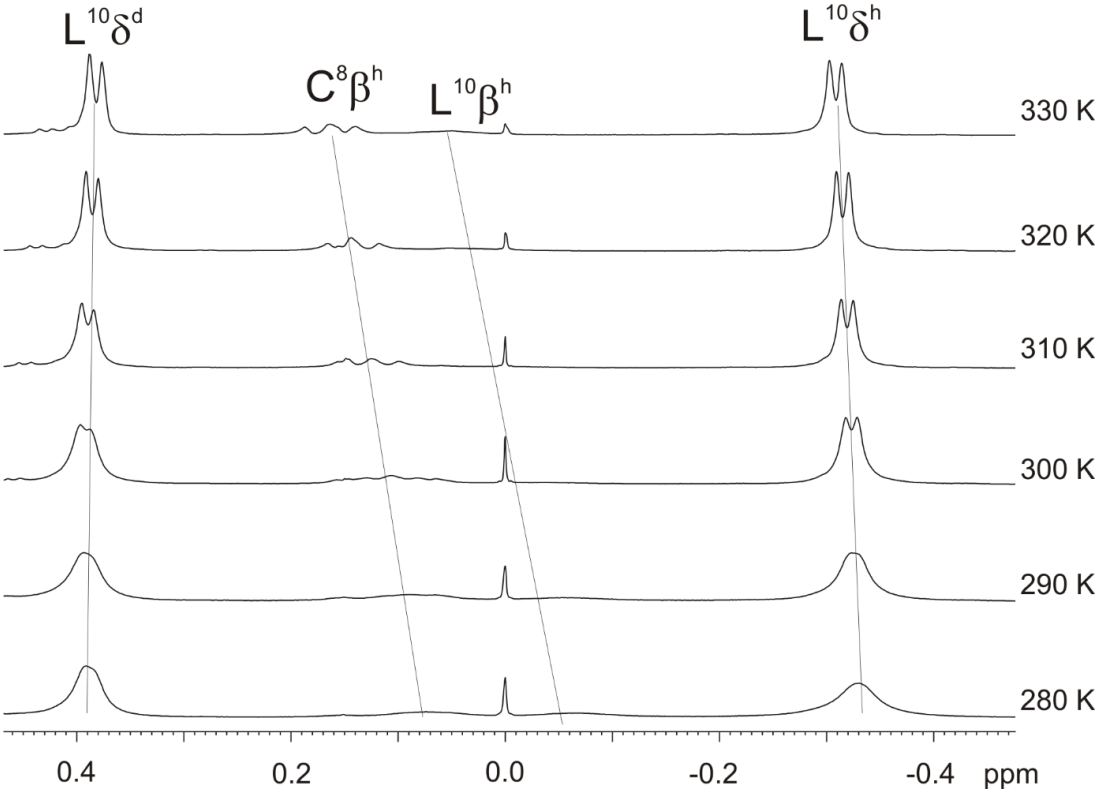

Figure S37. Leu-Hδ region of tetra-disulfide **1d** at different temperatures (600 MHz, 50 mM potassium phosphate buffer (pH 3.0)/D_2O 9:1). The spectra prove the integrity of the hydrophobic cluster and show that signal broadening decreases with increasing temperature. For comparison with the other dimers **2d** and **3d** see also figure S35.

NMR Comparison

The following figures S38-S40 show comparisons between the different dimers and between monomers and dimers respectively.

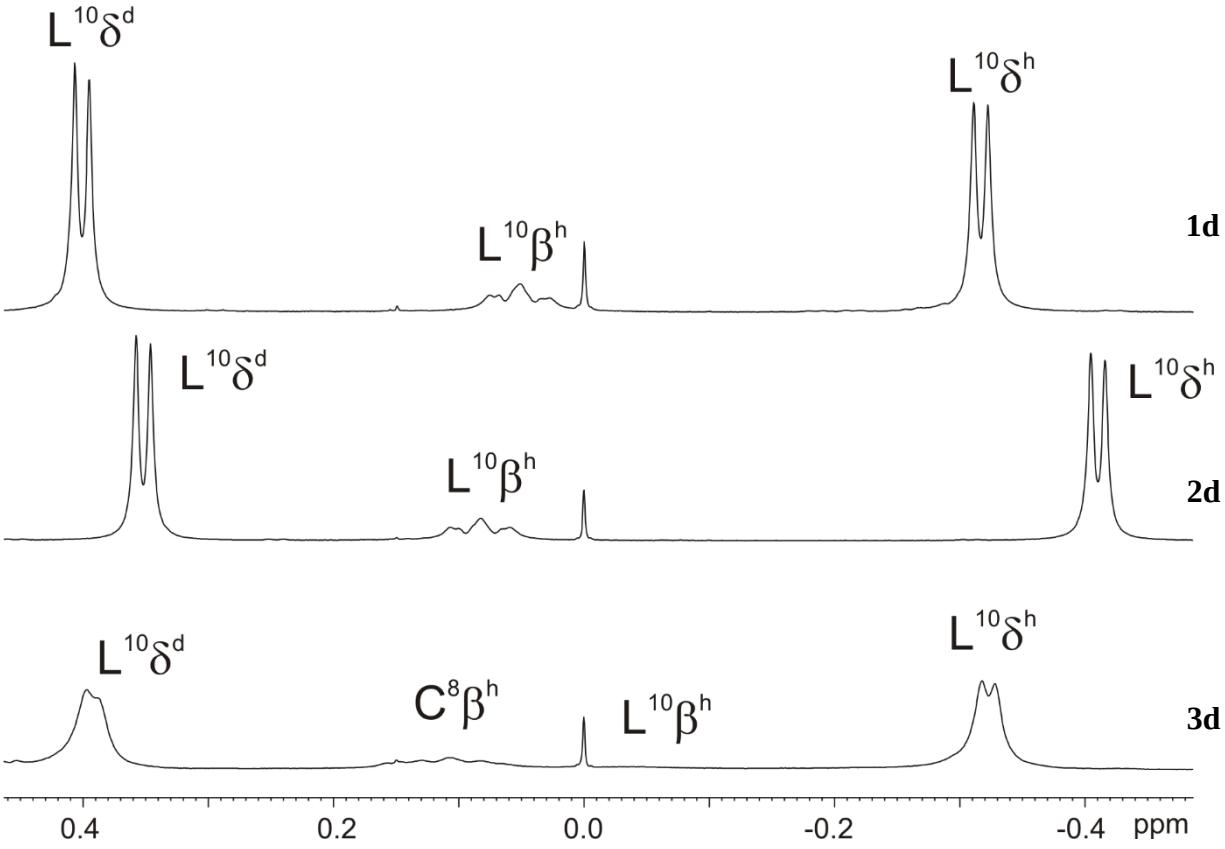

Figure S38. Comparison of the Leu-Hd region of dimers **1d**, **2d** and **3d** (600 MHz, 50 mM potassium phosphate buffer (pH 3.0)/D_2O 9:1).

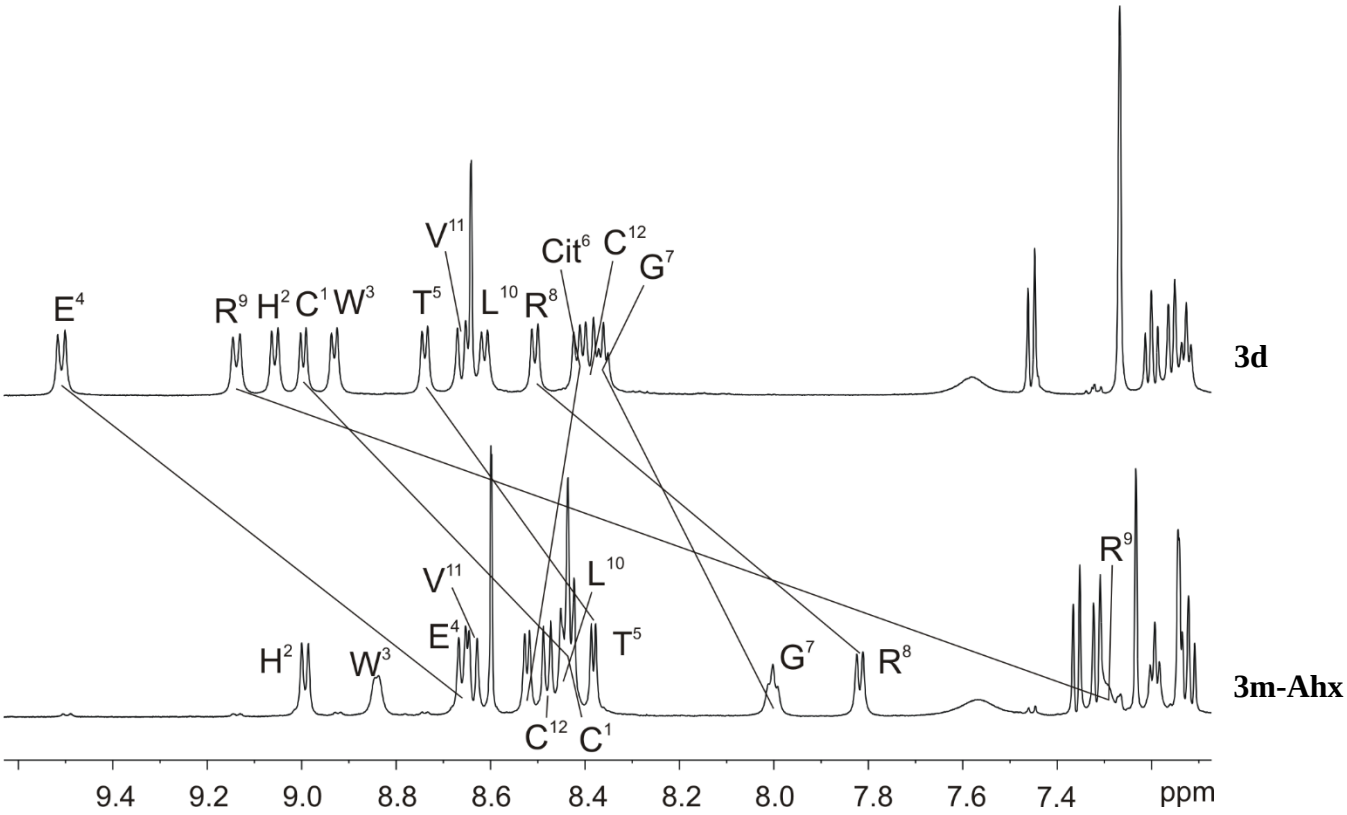

Figure S39. Comparison of the amide region of dimer **3d** (top) and monomer **3m-Ahx** (bottom) (600 MHz, 50 mM potassium phosphate buffer (pH 3.0)/D_2O 9:1).

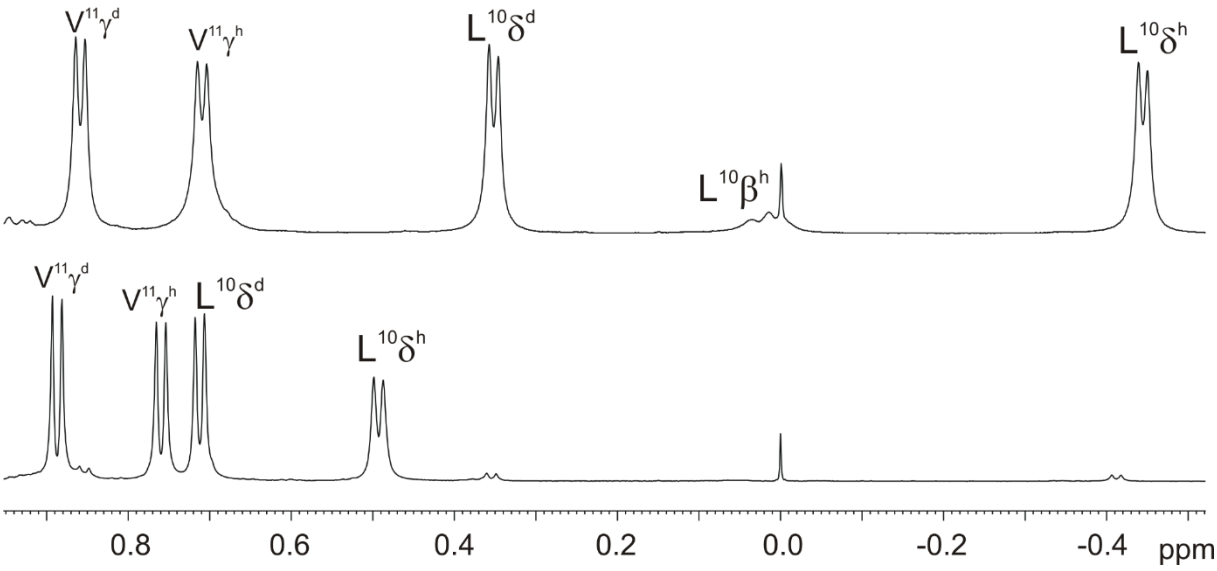

Figure S40. Comparison of the Leu-Hδ region of dimer **3d** (top) and monomer **3m** (bottom) (600 MHz, 50 mM potassium phosphate buffer (pH 3.0)/D_2O 9:1).

Backbone Interstrand NOEs

NOE contacts between the two strands of a β-hairpin verify an intact supersecondary structure. The spatial nature of the β-hairpin provides a specific order of Hα-Hα, Hα-NH, NH-NH and NH-Hα contacts. The corresponding excerpts from the NOE spectrum are shown exemplary for tetra-disulfide **1d** in figure S41-S43. A schematic depiction of the interstrand backbone NOE contacts is shown for all peptides (figure S44-S48).

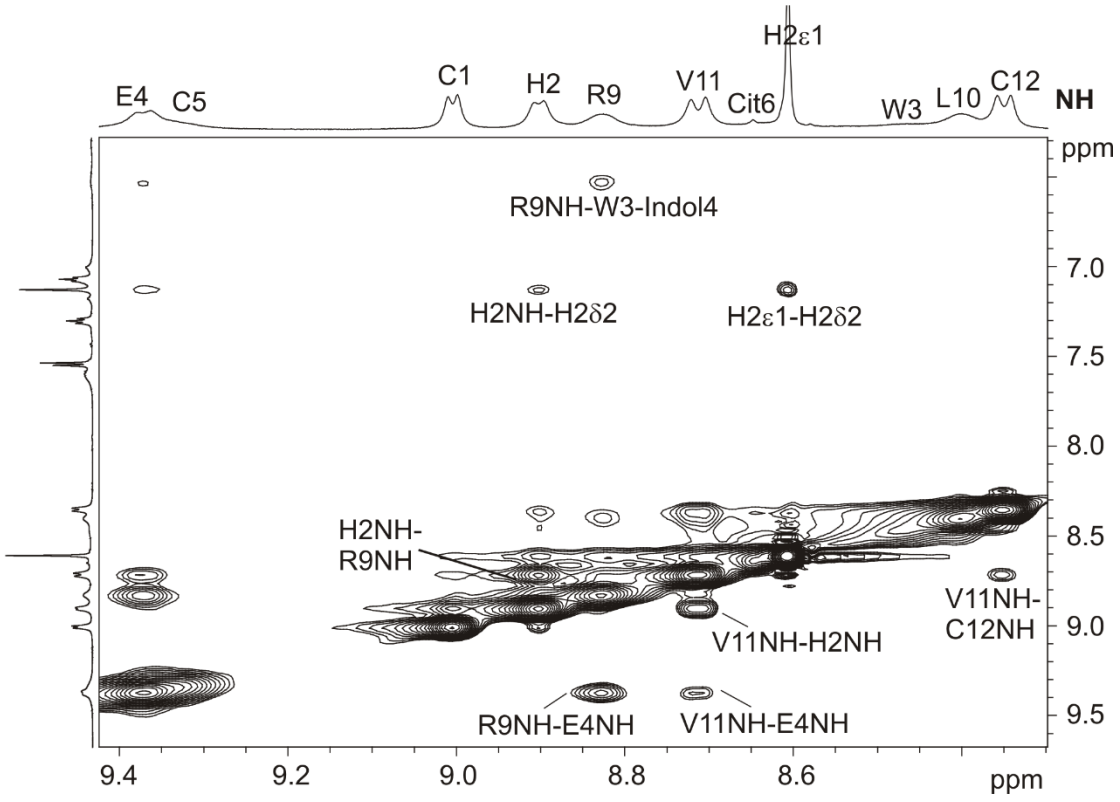

Figure S41. NH/NH NOE contacts for tetra-disulfide **1d**.

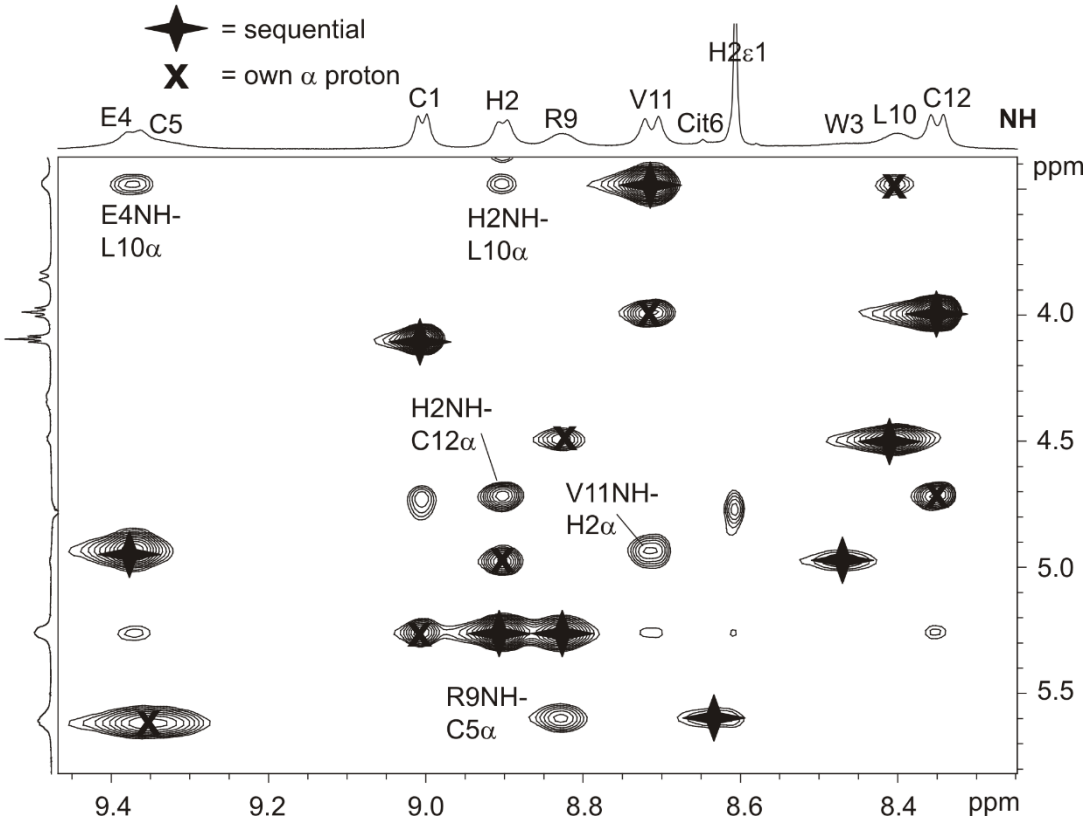

Figure S42. NH/α NOE contacts for tetra-disulfide **1d**.

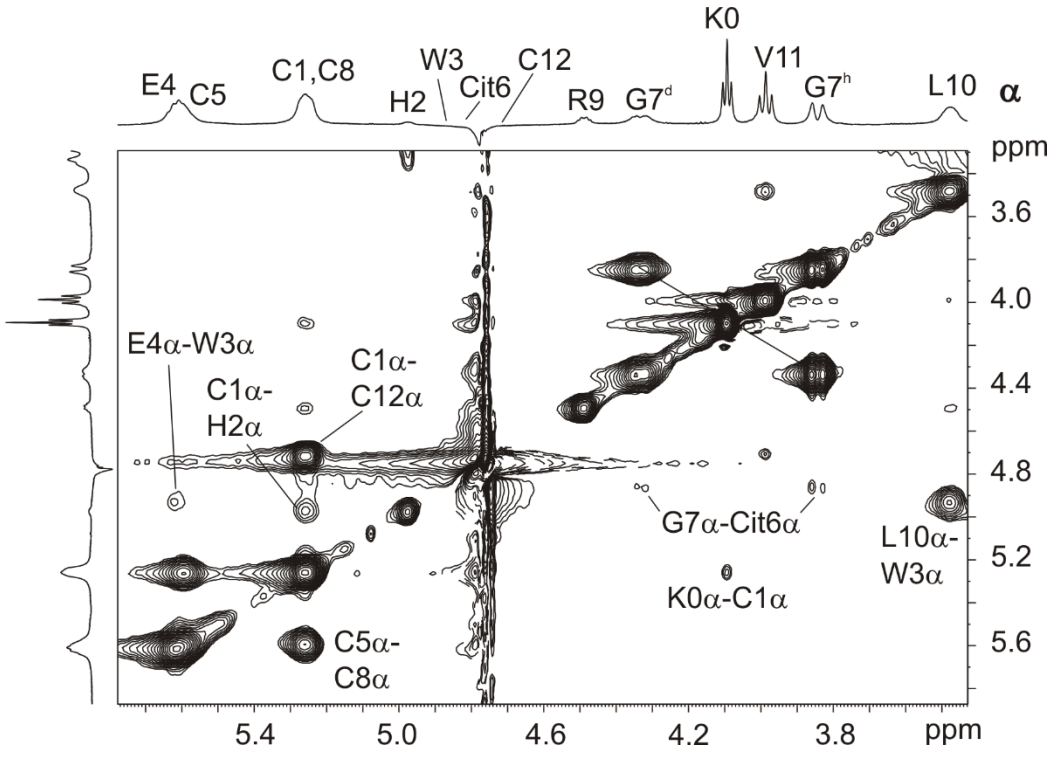

Figure S43. α/α NOE contacts for tetra-disulfide **1d**.

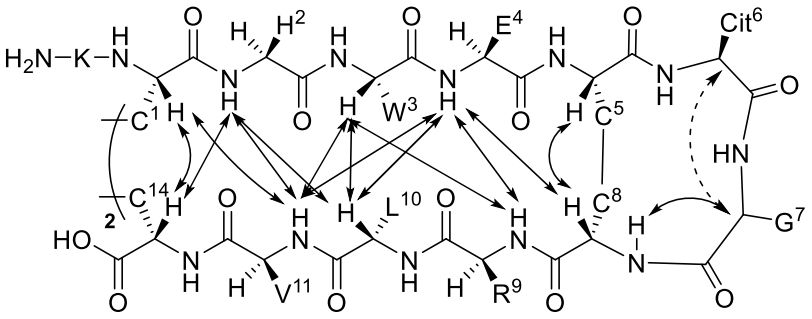

Figure S44. Backbone interstrand NOE contacts of tetra-disulfide **1d.**

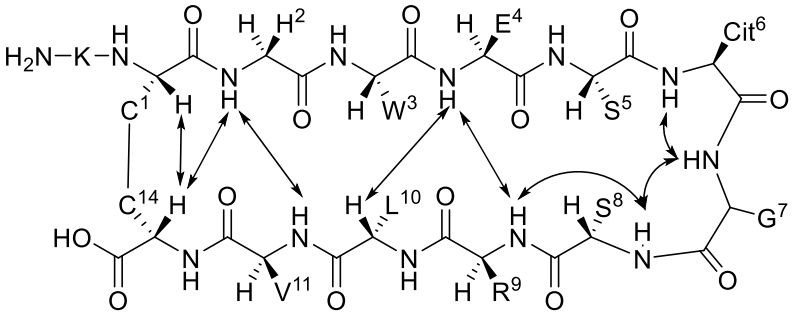

Figure S45. Backbone interstrand NOE contacts of monomer **2m.**

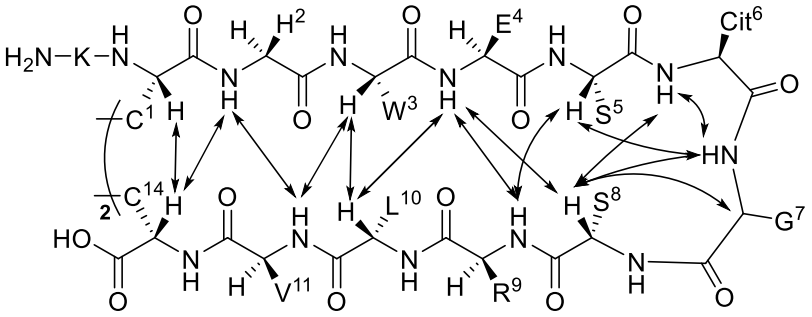

Figure S46. Backbone interstrand NOE contacts of dimer **2d.**

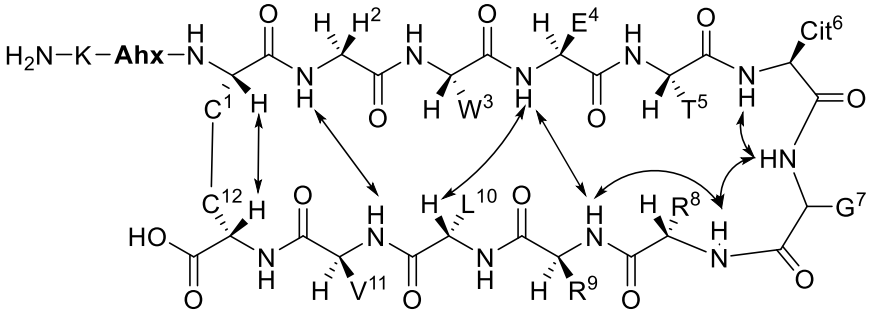

Figure S47. Backbone interstrand NOE contacts of monomer **3m-Ahx.**

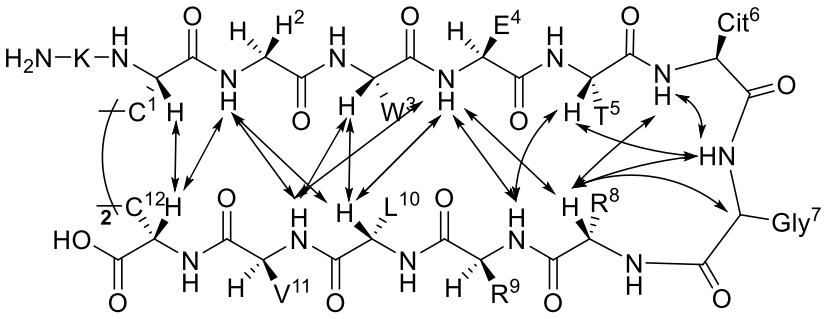

Figure S48. Backbone interstrand NOE contacts of dimer **3d.**

CD Spectroscopy

CD spectroscopy was run on a *Jasco J-810-150S* spectropolarimeter using the following parameters (pH was chosen equal to those of the NMR experiments):

- Peptide concentration: 200 μM in aqueous potassium phosphate buffer (2 mM, pH 7.0)
- Quartz cuvette path length: 0.1 cm
- Wavelength scanned: 260 nm - 190 nm
- Data pitch: 0.5 nm
- Response: 2 s
- Scanning speed: 10 nm/min
- Temperature: 300 K

Data from three consecutive scans were averaged and processed to improve the signal to noise ratio. The mean residue ellipticity (MRE in deg cm^2 $dmol^{-1}$) was calculated using the equation

$$\theta_{MRE} = \frac{\theta \cdot M_r}{c \cdot l \cdot n}$$

where θ is the measured ellipticity, M_r the molecular weight of the peptide, c the concentration of the sample, l the pathlength of the cuvette and n the number of peptide bonds. The CD spectra are found in the manuscript.

Ion Mobility Spectrometry

IMS measurements were done on a *Synapt G2-Si* (*Waters*). Experimental parameters have been adapted from literature-known procedures.[1,2]

Table S8. Experimental parameters for the ion mobility mass spectrometry measurements.[1,2]

ESI + V Resolution mode		DC potentials (V)		Traveling wave parameters	
m/z range	50 -2000	Trap Collision Energy	5	Source Wave Velocity (m/s)	300
Capillary (kV)	2.7	Transfer Collision Energy	0	Source Wave Height (V)	0.2
Source Temperature (°C)	70	Trap DC Entrance	3	Trap Wave Velocity (m/s)	300
Sampling Cone (V)	20	Trap DC Bias	40	Trap Wave Height (V)	5
Extraction Cone (V)	5	Trap DC	-1	IMS Wave Velocity (m/s)	350
Source Gas Flow (mL/min)	20	Trap DC Exit	0	IMS Wave Height (V)	20
Desolvation Temperature (°C)	250	IMS DC Entrance	25	Transfer Wave Velocity (m/s)	350
Cone Gas Flow (L/hr)	0	Helium Cell DC	35	Transfer Wave Height (V)	5
Desolvation Gas Flow (L/hr)	500	Helium Exit	-5		
Trap Gas Flow (mL/min)	0.4	IMS Bias	0		
Helium Cell Gas Flow	180	IMS DC Exit	0		
IMS Gas Flow (mL/min)	70	Transfer DC Entrance	4		
Sample Infusion Flow Rate (µL/hr)	300	Transfer DC Exit	15		

The spectrometer was calibrated on the basis of the drift-tube derived collisional cross sections (CCS) of doubly and triply protonated polyalanine using the method of BUSH *et al.*[3] Thus, CCS can be estimated from measured TWIM (travelling wave ion mobility) drift times.

Table S9. Obtained drift times and CCS values for monomers and dimers at different charge states. The CCS values have been calculated from drift times and corresponding peptide mass and charge states.

	Drift time / ms					CCS / Å²				
Peptide	**z = 1**	**z = 2**	**z = 3**	**z = 4**	**z = 5**	**z = 1**	**z = 2**	**z = 3**	**z = 4**	**z = 5**
1d (C5,C8)	n/a	n/a	7.17	4.62	4.20	n/a	n/a	644	685	n/a
2d (S5,S8)	n/a	n/a	7.65	4.82	n/a	n/a	n/a	667	703	n/a
3d (T5,R8)	n/a	n/a	7.65	5.17	4.00	n/a	n/a	669	727	797
2m (S5,S8)	7.92	6.68	n/a	n/a	n/a	228	418	n/a	n/a	n/a
3m-Ahx (T5,R8)	11.99	7.72	4.34	n/a	n/a	281	449	503	n/a	n/a

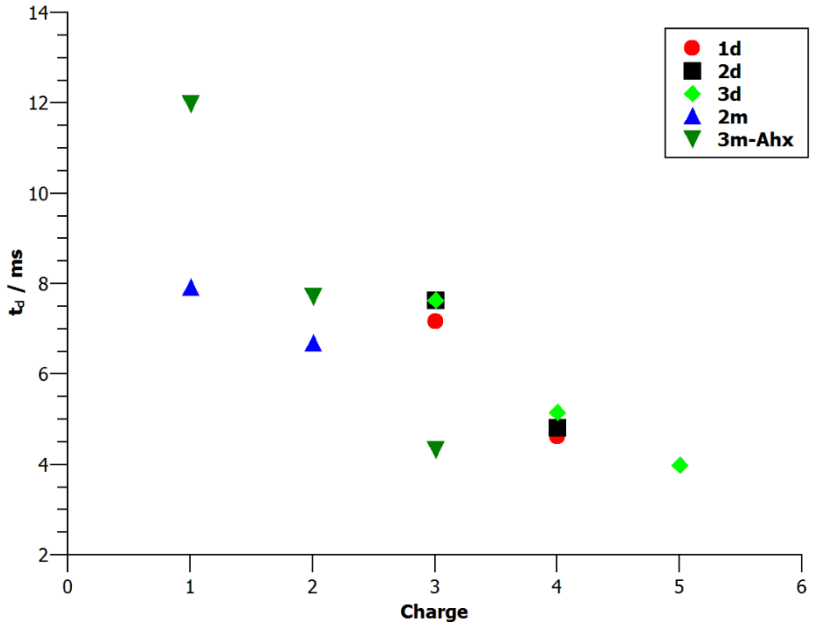

Figure S49. Plot of the peptide charge state (x-axis) with corresponding drift times (d_t).

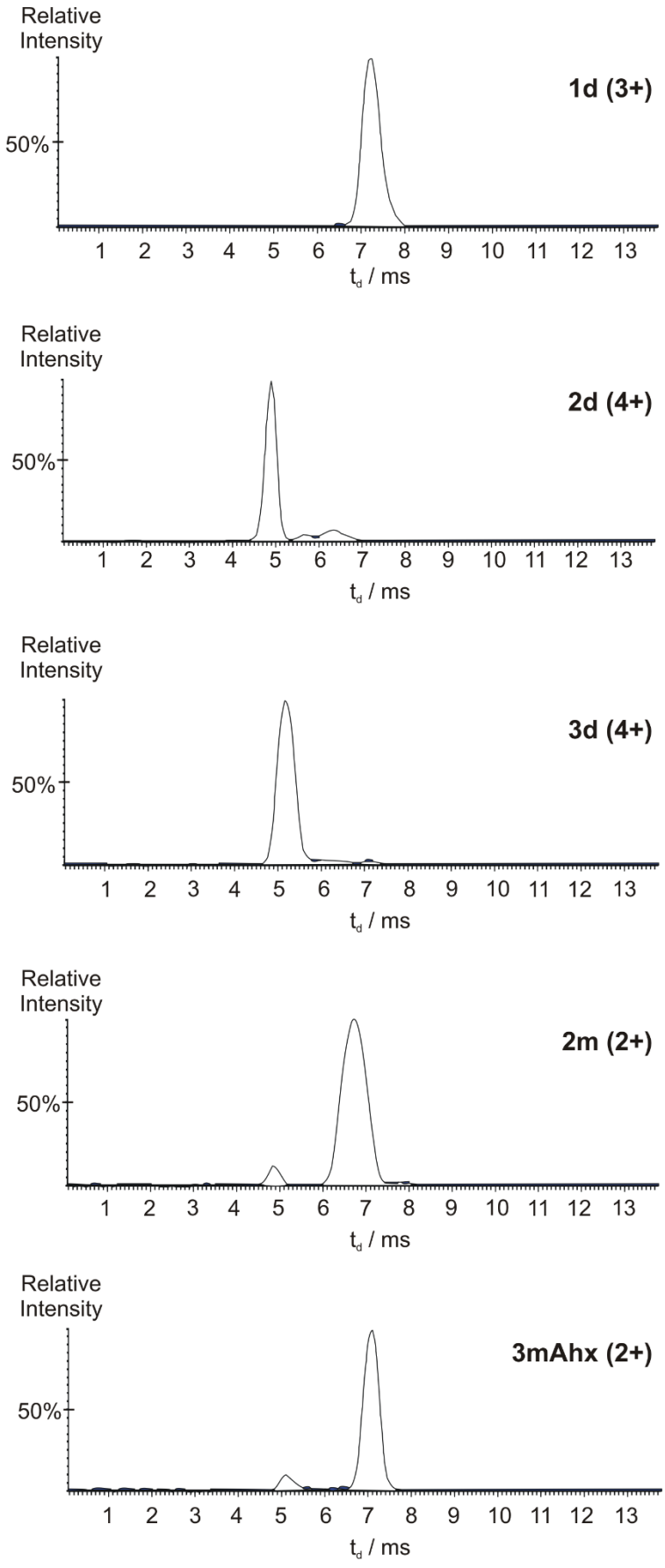

Figure S50. Ion mobility spectra of the denoted peptides with corresponding charge state.

Interpretation

Drift times are substance specific parameters for every peptide under the same experimental parameters (table S8). They are dependent on mass, charge state and the spatial arrangement of the macrocycles. As similar to equal drift times are achieved among the dimers and among the monomers (with almost the same mass and equal charge state), the peptides' conformations should closely resemble each other. Accordingly, the calculated collisional cross sections (CCS or **Ω**) are similar among the particular peptide species, proving the validity and the reproducibility of the method in iterative experiments.

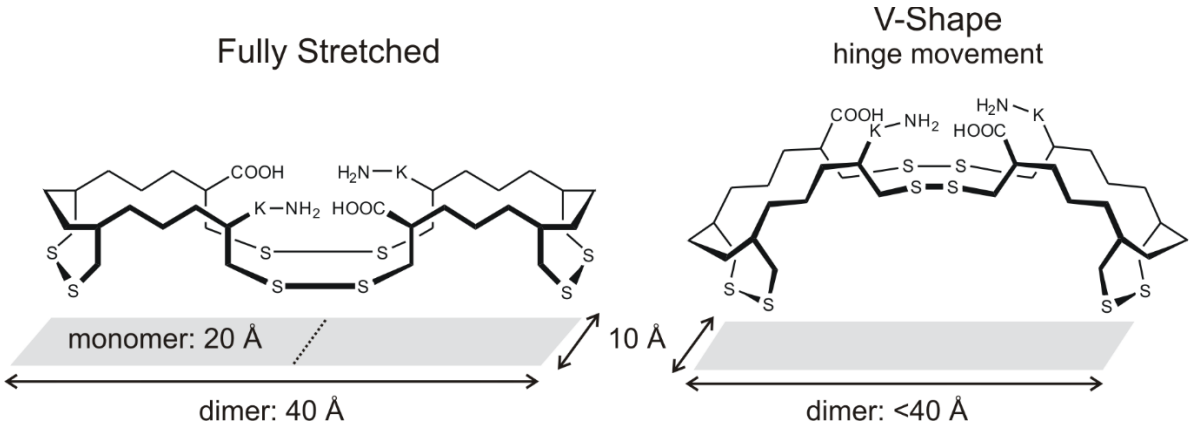

Figure S51. Simplified depiction of the hinge movement of the dimeric epitope with corresponding altered projection area (collision cross sections)

The length of the hairpin structures is limited by the possible bond lengths and geometries, leading to values of around 20 Å (from C1Hβ to Cit6Hα) for the monomer or 40 Å for the dimers (from Cit6Hα to Cit6'Hα) in a fully stretched conformation (derived from molecular dynamics simulation, compare figure S51). The width of the peptides has likewise been inferred to be around 10 Å maximum. As CCS values describe the projection area of the peptide, this area can consequently be not much larger than 200 $Å^2$ for the monomers and 400 $Å^2$ for the dimers. Thus, the calculated CCS from our obtained drift times do not reflect the absolute, chemically possible values of monomers and dimers, which can only be explained by the completely different structural properties of the polyalanine species, that were used for calibration. The CCS is related to to the mobility of the measured ion via the MASON-SCHAMP equation (1):[4]

$$\Omega = \frac{3ze}{16N} \cdot \left(\frac{2\pi}{\mu k_B T}\right)^{\frac{1}{2}} \cdot \frac{1}{K} \quad (1)$$

Ω: CCS, z: charge, e: elementary charge, N: number density of the drift gas, μ: reduced mass of the drift gas, k_B: Boltzmann constant, T: gas temperature, K: mobility of the measured ion

The ion mobility is connected with the drift time via equation (2), where t_0 strongly depends on m/z:

$$t_D = \left(\frac{l_{dc}}{KE}\right) + t_0 \quad (2)$$

t_D: drift time, l_{dc}: length of the drift cell, K: mobility of the measured ion, E: electric field, t_0: transport time of ions from the exit of the drift cell to the mass analyser.

Assuming similar molecular masses and the same charge states, the compact hairpin structure of our peptides leads to a fundamentally altered distribution of positive charges over the peptide backbone and thus different drift behaviour. Consequently, CCS values are correlated with those of random coil polyalanine derivatives with comparable mass and charge but actually higher CCS (for the same drift time), delivering projection areas that are comparatively too high for otherwise substance specific and reproducible drift times. Put the other way around, a more globular polyalanine derivative must supposedly adopt a far higher CCS for the same drift time than a shape-persistent, less globular hairpin structure.

Despite these facts, the relative comparison of the CCS values is still valid. While monomers and dimers show equal to similar CCS values among each other, the comparison between monomer and dimer is of special interest as it delivers information about the hinge movement of the dimers, which can adopt fully stretched (180°) or V-shaped arrangements (<180°). We therefore compared twofold charged monomers with fourfold charged dimers to calculate with the same charge distribution per monomer fragment. The relation of the CCS of dimer(4+)/monomer(2+) yielded a factor of 1.7. This finding indicates that the dimer's projection area is indeed smaller than the potential twofold monomer CCS and should exhibit a length of around 34 Å. Thus, IMS is an excellent method to access the hinge movement of the dimers.

Molecular Dynamics Simulation

The modelling of **1d** was carried out as described previously[5,6] using the program package *HyperChem* with the MM+ force field but without explicit water.[7] NOE, hydrogen bond, and side chain torsional restraints were derived from the experimental NMR data and included as target values in the modelling. The final structure shown in Fig. 9 was obtained after energy minimisation.[8]

References

1 K. Jeanne Dit Fouque, C. Afonso, S. Zirah, J. D. Hegemann, M. Zimmermann, M. A. Marahiel, S. Rebuffat and H. Lavanant, *Anal. Chem.*, 2015, **87**, 1166–1172.

2 K. J. D. Fouque, H. Lavanant, S. Zirah, J. D. Hegemann, M. Zimmermann, M. A. Marahiel, S. Rebuffat and C. Afonso, *J. Am. Soc. Mass Spectrom.*, 2016.

3 M. F. Bush, I. D. G. Campuzano and C. V. Robinson, *Anal. Chem.*, 2012, **84**, 7124–7130.

4 E. A. Mason and E. W. McDaniel, *Transport Properties of Ions in Gases*, Wiley, New York, 1998.

5 S. Enck, F. Kopp, M. a Marahiel and A. Geyer, *ChemBioChem*, 2008, **9**, 2597–2601.

6 M. Haack, S. Enck, H. Seger, A. Geyer and A. G. Beck-Sickinger, *J. Am. Chem. Soc.*, 2008, **130**, 8326–8336.

7 HyperChem, Hypercube, Inc., Gainesville, FL, 2000.

8 W. L. DeLano, The PyMOL Molecular Graphics System, DeLano Scientific LLC, San Carlos, CA, 2008.